Petrography and Mineral chemistry of Archaean Metapelites from Eastern Dharwar Craton, Southern India.

Dr. N. Mahesha

Department of Civil Engineering, New Horizon College of Engineering,

Abstract— In this paper an attempt has been made to present petrography and chemical data for the principal minerals (biotite, cordierite, garnet, orthoamphibole, orthopyroxene, sillimanite, plagioclase and spinel) of the metapelites from different localities in the Eastern Dharwar Craton viz., Pavagada, Bidaloti and Bandihalli areas to bring out the differences, similarities and petrogenetic significance of these minerals from one locality to another. At the end of the paper, various geothermobarometric models are used to quantify the pressure-temperature conditions of metamorphism in the Eastern Dharwar Craton.

Keywords— Petrography, Metapelites, Eastern Dharwar Craton, Pressure-temperature conditions, Metamorphism

I. INTRODUCTION

There is a progressive change in the grade of regional metamorphism from North to South in the Dharwar craton (Rama Rao, 1936). The earlier work (Pichamuthu, 1985; Janardhan et al., 1982; Raith et al. 1982; Hansen et al., 1984; Raase et al. 1986; Bouhallier, 1995) on this aspect suggest that the grade of metamorphism varies from greenschist facies in the north and amphibolite facies to granulite facies in the South. Pichamuthu (1985) attributed this increase in metamorphic grade to increasing depth of burial. By studying the mineral chemistry of potash feldspar, garnets and amphiboles, a southward increase in regional metamorphism was proposed (Anantha Iyer and Narayana Kutty, 1974) while Radhakrishna (1984) and Swami Nath and Ramakrishnan (1981) have reported two basic types of metamorphic facies, on the western side of Closepet granite an intermediate pressure and on the eastern side low pressure metamorphism. The low pressure metamorphism in the eastern block is attributed to granites of Closepet and differing crustal thickness (Swami Nath and Ramakrishnan 1981). On the other hand Swami Nath et al (1976) and Rollinson et al (1981) have documented contrasting metamorphic assemblages in the western and eastern block. Despite numerous attempts on addressing issues related to the amphibolites-granulite transition, particularly at the type area of Kabbaldurga (Janardhan et al., 1982; Raith et al., 1982; Hansen et al., 1984), the significance of the observed north-south metamorphic gradient are of the contrasting nature of metamorphism in the Western Dharwar Craton and Eastern Dharwar Craton remain elusive. In this context we have studied petrography and mineral chemistry of metapelites of different localities from Eastern Dharwar Craton viz., Pavagada, Bidaloti and Bandihalli areas (Fig. 1) to understand Mineral reactions, equilibrium mineral assemblages and pressure-temperature conditions of metamorphism in the Eastern Dharwar Craton.

II. GEOLOGICAL SETTINGS

The Archaean crust in the EDC comprises 2.7 - 2.6 Ga TTG-greenstone associations with minor remnants of >3.0 Ga basement enclaves (TTG and interlayered high grade supracrustal rocks) and most voluminous roughly north-south trending late 2.56 - 2.52 Ga calc-alkaline to potassic composite plutons (Krogstad et al., 1991; Friend and Nutman, 1992; Peucat et al., 1993; Nutman et al., 1996; Jayananda et al., 2000; Chardon et al., 2002). The most spectacular of these composite plutons is the 2.52 Ga old 400 km long, N-S trending Closepet granite (Jayananda et al., 1995, 2000). Several small discontinuous bands of high grade supracrustal rocks (quartzites – metapelites - calc silicate – amphibolite - BIF) floating in TTG country rocks are found mostly along the periphery of the Closepet granite. These supracrustal rocks are mainly confined to interfering regional NNE-trending dextral and NNW-trending sinistral shear zones (Chardon et al., 2008) and are well exposed around Pavagada, Bidaloti and Bandihalli areas. Out of these supracrustal rocks we are focussed only on metapelites for the current study.

The Pavagada area is located in the Central part of the EDC along the eastern boundary of the Closepet granite (Fig. 1). The studied metapelites found as NE trending bouldary exposures, with large porphyroblasts of sillimanites with relict blades of kyanites. These metapelites are weakly migmatized and injected by tiny granitic veins. Migmatization and injection of granite veins are contemporaneous as melt accumulation can be observed along shear bands. Thin film of melt found around sillimanite/Kyanite porphyroblasts indicates development sillimanite/kyanite prior to migmatization.

Bidaloti area is located along eastern boundary of the Closepet granite (Fig. 1). The studied metapelites occur as bouldary exposures and show N 5-10^0 E trending foliation. They are dark grey coloured and show weak migmatization, where melt accumulation as thin veins along shear bands can be observed. These metapelites are injected by Closepet granite veins.

The Bandihalli area is situated on the western margin of the Closepet granite (Fig. 1). The metapelites of the area are represented by cordierite-anthophyllite-garnet-biotite schist, and biotite-quartz-schist. These are widely exposed in the southern portions of the area and are sporadic in the northern portions. The striking feature of the metapelites is that most of the minerals are well developed and also show migmatitic character.
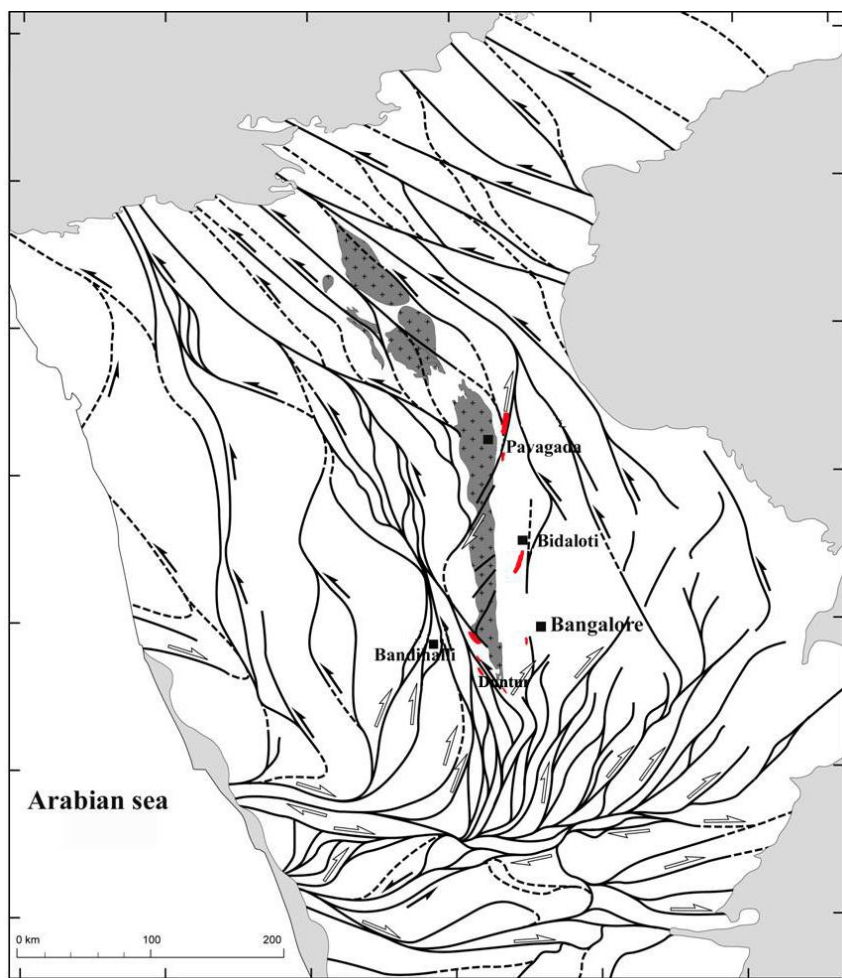
Fig. 1. Bird eye view of the studied areas bordering around Closepet granite (after Chardon et al 2008).

III. PETROGRAPHY

We have studied nearly 50 samples of metapelites from Pavagada, Bidaloti & Bandihalli areas and photomicrographs were taken by using Leica DMRXP petrological microscope at Geological Survey of India, Bangalore. The area wise, detailed petrographic descriptions were described below;

Pavagada Area: Based on mineral associations three varieties of metapelites have been identified.
1. Sillimanite + cordierite + spinel + biotite + plagioclase + quartz.
Sillimanite, biotite and cordierite occur as porphyroblastics phases. Prismatic sillimanite and biotite show strong preferred orientation. Spinel is characteristically granular and devoid of intergrowth magnetite and clusters around/along the margins of sillimanite prisms (Fig. 2). Granular spinel is intergrown with cordierite (Fig. 3), but quartz is absent in the intergrowths. Subhedral prophyroblasts of cordierite occur additionally in the rock, which is not intergrown with spinel. Textural features establish that early stabilized biotite and sillimanite and quartz gave way to an assemblage of spinel and cordierite according to the reaction, Biotite + sillimanite + quartz ---------------- cordierite + spinel + H_2O/melt.
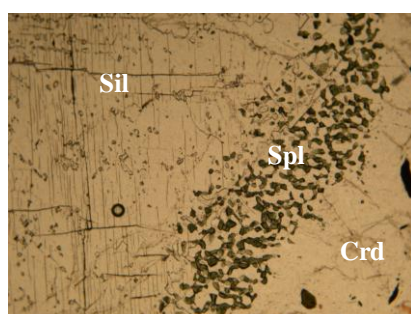

Fig. 2. Granular spinel clusters devoid of intergrowth magnetite around/along the margins of sillimanite prisms.
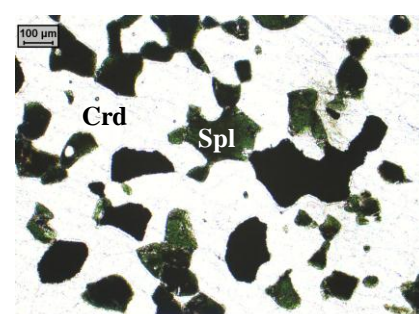

Fig.3. Granular spinel intergrowth with cordierite.

2. Cordierite + orthopyroxene + plagioclase + biotite + garnet + sillimanite + spinel + quartz + ilmenite + magnetite.

This association is characterized by the occurrence of porphyroblastics cordierite and orthopyroxene with substantial amount of coarse ilmenite and minor magnetite. Since the cordierite is showing unusual optical characters than normal cordierite, XRD studies were carried out, which indicate that the cordierite is a sub-distortional cordierite (Fig. 14). Plagioclase is restricted to inclusions within orthopyroxene and cordierite, while biotite occurs both as inclusions in orthopyroxene and as patches along the grain boundaries of the latter. Garnet occurs in a variety of size and shape. Besides occurring as scattered medium sized grains, it occurs as thick coronae around cordierite and orthopyroxene. Garnet is further intergrown with worm-like spinel and magnetite (Fig. 4). Spinel also occurs as relatively coarse grains invariably at the grain boundaries of garnet (Fig. 5). Early stabilization of porphyroblastic cordierite and orthopyroxene, along with plagioclase and quartz, can be related to breakdown of biotite, plagioclase and quartz in a semi-pelitic/psammopelitic protolith (note the absence of primary sillimanite),

Biotite+plagioclase+quartz………………orthopyroxene+cordierite+K-feldspar+H_2O
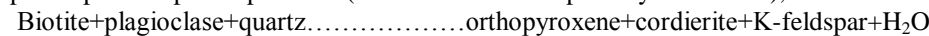
Garnet probably appeared through multiple reactions. The medium sized grains in the matrix showing no relationship with orthopyroxene or cordierite could have been produced by the reaction,

Biotite+plagioclase+quartz………………garnet+K-feldspar+H_2O

Garnet also appeared subsequently in the association through a reaction between porphyroblastic orthopyroxene and cordierite (Fig. 6) that also produced coronal sillimanite,

Orthopyroxene+cordierite………garnet+sillimanite.
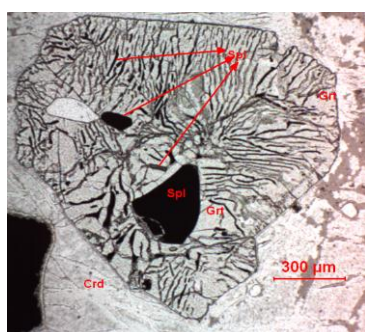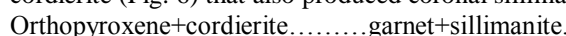
Fig. 4. Garnet intergrown with worm-like spinel and magnetite.
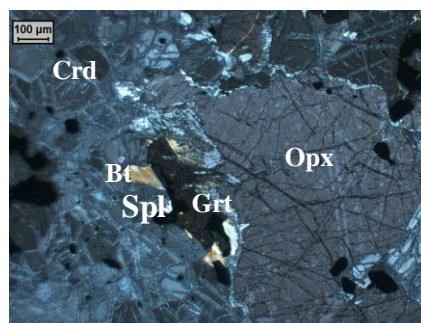
Fig.5. Spinel occurs as relatively coarse grains invariably at the grain boundaries of garnet.
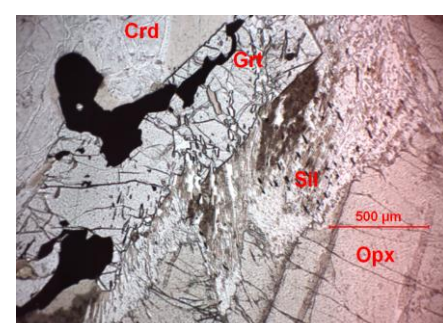
Fig.6. Garnet appeared subsequently through a reaction between porphyroblastic orthopyroxene and cordierite.

The occurrence of work-like intergrowth between garnet and spinel (Fig. 4) is enigmatic. Das et al. (2006) described similar intergrowths from the ultrahigh temperature metamorphosed Eastern Ghats Belt and offered several alternative explanations. One of the possibilities mentioned by Das et al. (2006) is due to decomposition of a highly aluminous orthopyroxene. In the present occurrence, orthopyroxene is not as aluminous as the case described by them, neither is there any evidence of such ultrahigh temperature metamorphism. We prefer the alternative explanation given by Das et al. (2006) that the intergrowth spinel could be pseudomorphous after included sillimanite and was formed due to the reaction, Garnet+sillimanite…………………spinel+quartz.

This is supported by the occurrence of spinel along the grain boundaries of garnet (Fig. 5). Retrograde low Ti-biotite developed subsequently due to hydration of the assemblage.

3. Cordierite + plagioclase + orthoamphibole + biotite + orthopyroxene + quartz.

Sillimanite is totally absent in this association, which is characterized by the appearance of porphyroblastic cordierite and plagioclase and minor quartz, orthoamphibole (anthophyllite) and biotite. Orthoamphibole replaces orthopyroxene along the grain boundaries. Biotite occurs as an inclusion phase in cordierite and orthopyroxene, but also replaces the latter. The following reaction is responsible for production of porphyroblastic cordierite and orthopyroxene,

Biotite+plagioclase+quartz………………orthopyroxene+cordierite+K-feldspar+H_2O.
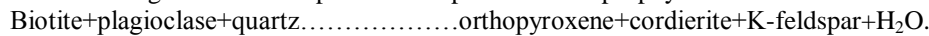
Orthoamphibole developed due to hydration of orthopyroxene according to the reaction,

Orthopyroxene+quartz+H_2O………………anthophyllite.
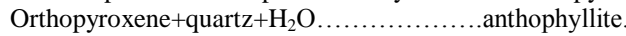
Bidaloti area: Based on mineral assemblages two varieties of metapelites have been identified.

1. Orthopyroxene (opx) + anthophyllite + biotite + cordierite + Quartz.

The rock shows granulitic texture. Orthopyroxene occur in various shapes, as tabular plates with good crystal outlines or as small anhedral grains which are feebly pleochroic. Anthophyllite mantles opx suggesting hydration reaction (Fig. 7),

Orthopyroxene+quartz+H2O………………anthophyllite.

Biotite is deep brown in colour and occurs as large flakes. Cordierite is found as anhedral grains and contains pleochroic haloes. Quartz occurs as xenoblastic grains. The opx, cordierite, anthophyllite, biotite contacts are lobate and hence may be equilibrium assemblages.

2. Opx + spinel + cordierite + anthophyllite + phlogophite + quartz.

The rock exhibits xenomorphic granular texture. Orthopyroxene occur as small anhedral grains and are feebly pleochroic. Anthophyllite occurs as elongated grains showing well developed cleavages and straight extinction (Fig. 8). Cordierite is

strewn with tiny magnetite inclusions and has pleochroic haloes. The grain boundary between opx-cordierite and anthophyllite are lobate suggesting equilibrium assemblages. The spinel occurs as inclusion and also as vermicular grains within cordierite (Fig. 9). Minor amount of quartz occurs as anhedral grains.
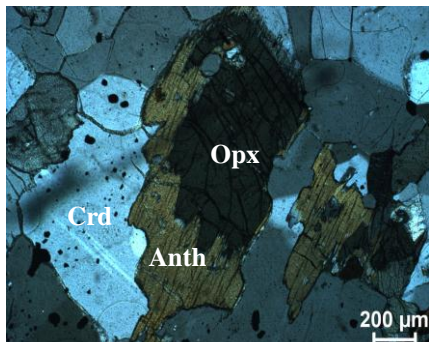

Fig. 7. Anthophyllite mantles opx.
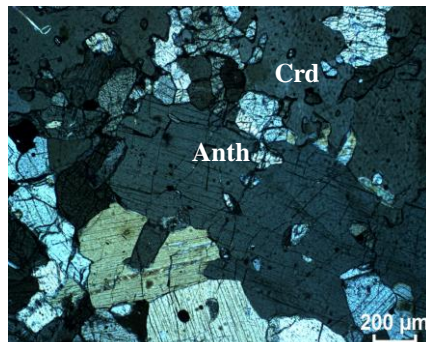
Fig. 8. Anthophyllite occurs as elongated grains showing well developed cleavages.
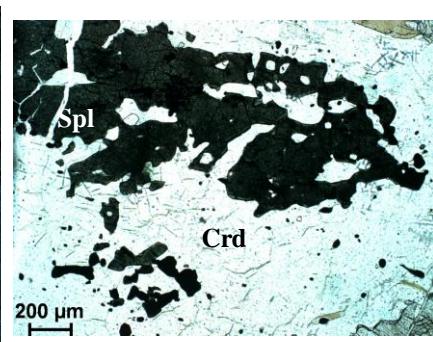
Fig. 9. Spinel occurs as inclusion and also as vermicular grains within cordierite.

Bandihalli area: Based on mineral assemblages two varieties of metapelites have been identified.
1. Anthophyllite + cordierite + biotite+sillimanite.
In thin section the rock exhibits schistose texture. Anthophyllite occur as sheaves and shows preferred orientation (Fig. 10). Cordierite occurs as plates, showing pleochroic haloes. Biotite occurs as laths and is wrapped around anthophyllite (Fig. 11). Sillimanite occurs as slender prismatic crystals or as needles. It is slightly pleochroic from colourless to light green and exhibit parallel extinction. However, the probable mineral reactions deduced from the texture is, Biotite + sillimanite + quartz ……………..   anthophyllite + cordierite + melt.

2. Anthophyllite + cordierite + biotite + garnet.
In thin section the rock exhibits schistose texture with anthophyllite showing preferred orientation. Garnet occurs as porphyroblasts and is wrapped by biotite (Fig. 12). Biotites occur as laths. Cordierite found as anhedral plates with pleochroic haloes. Textural evidence suggest the following reaction,
Anthophyllite + cordierite……………….. garnet + gedrite.
The reactions suggested for both the types are coupled reactions as both reactants and products coexist in the rock.
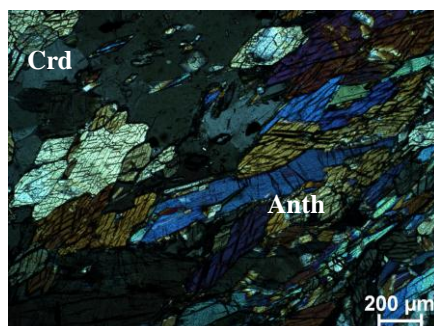
Fig. 10. Anthophyllite occur as sheaves and shows preferred orientation
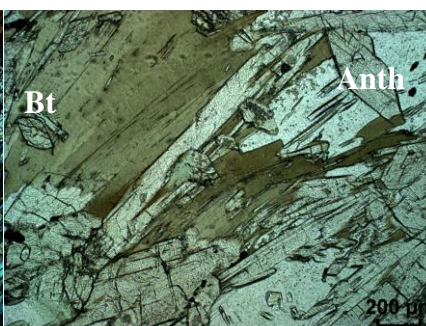
Fig. 11. Biotite occurs as laths and is rimmed around anthophyllite.

Fig. 12. Porphyroblastic garnet rimmed by biotite.

IV. **MINERAL CHEMISTRY**

Chemical compositions of the various minerals were determined by using a JEOL-JXA-8600 electron microprobe at Yamaguchi University, Japan and with a CAMECA SX-50 Electron Probe Microanalyzer (EPMA) at the Petrological Laboratory of Geological Survey of India, Kolkata. The chemical data of the principal minerals of the studied metapelites were presented in the following paragraph.

Biotite: The chemical data of biotite of all the studied area metapelites is presented in the Table I. The structural formulas were calculated on the basis of 11 (O) atoms. All Fe is calculated as Fe^{2+}. The sum of Si and Al always exceeds 4. All the Biotites are more aluminous, having variable Al^{iv} content. The TiO_2 content in the biotites of Pavagada area vary from 3.26- 4.51wt%, Bidaloti area vary from 2.06-3.85wt% and Bandihalli area vary from 1.58-1.92 wt %. Generally, all the biotites are poor in MnO, CaO and Na_2O. High Ti and low Mn contents of biotites indicate higher grade of metamorphism, amphibolite to granulite facies transition (Horman et al., 1980; Dymek, 1983; Hansen et al., 1984a, b). On Ti Vs X_{Mg} diagram (Fig. 13) the biotites of Pavagada area plot in the field of annite whereas the biotites of Bidaloti and Bandihalli area plot in the field of phlogopite.

Table. I. Chemical analysis of Biotite.

Area	Pavagada																	
Sample No.	P-01					P-10					P-11		P-14				P-16	
Oxides	11	15	19	29	30	29R	30C	31	38	39	4	9	7C	16R	17C	19	19	20
SiO_2	36.87	35.69	36.08	39.28	37.68	36.94	36.92	37.07	37.21	37.18	35.76	35.83	35.01	34.70	37.33	35.98	33.58	35.10
TiO_2	3.73	3.66	3.72	3.76	3.65	3.38	3.38	3.36	3.48	3.48	3.45	3.26	3.29	3.44	3.58	3.84	3.65	3.64
Al_2O_3	17.84	17.93	16.83	17.98	17.87	16.35	16.60	16.24	16.62	16.62	16.31	15.85	16.64	18.18	17.10	16.38	18.73	18.97
Cr_2O_3	0.35	0.39	0.38	0.57	0.57	0.61	0.45	0.52	0.00	0.54	0.82	0.85	0.46	0.54	0.53	0.60	0.50	0.65
FeO	17.56	17.83	17.84	18.37	17.17	16.71	17.06	17.84	17.31	17.31	16.59	16.69	16.51	15.72	16.30	16.29	16.74	17.15
MnO	0.05	0.05	0.06	0.04	0.05	0.01	0.09	0.06	0.02	0.02	0.01	0.03	0.00	0.11	0.05	0.04	0.05	0.11
MgO	9.83	9.90	9.81	10.55	10.11	11.63	11.90	11.47	11.93	11.94	12.32	11.97	13.42	12.64	12.99	12.72	10.66	10.49
CaO	0.00	0.00	0.00	0.00	0.00	0.00	0.00	0.00	0.01	0.01	0.00	0.00	0.00	0.00	0.00	0.01	0.00	0.00
Na_2O	0.21	0.17	0.17	0.21	0.25	0.22	0.16	0.14	0.21	0.21	0.21	0.14	0.13	0.14	0.18	0.18	0.31	0.28
K_2O	9.36	9.37	8.54	9.46	9.13	9.53	9.98	9.85	9.71	9.70	9.26	9.46	9.01	8.79	9.65	9.47	9.75	9.56
Total	95.80	94.99	93.43	100.21	96.49	95.39	96.52	96.53	96.50	97.01	94.72	94.08	94.47	94.26	97.72	95.51	93.95	95.96
Cation Numbers based on (O) 11																		
Si	2.76	2.71	2.77	2.80	2.79	2.78	2.76	2.77	2.77	2.76	2.72	2.74	2.66	2.63	2.73	2.71	2.59	2.64
Ti	0.21	0.21	0.21	0.20	0.20	0.19	0.19	0.19	0.20	0.19	0.20	0.19	0.19	0.20	0.20	0.22	0.21	0.21
Al	1.57	1.60	1.52	1.51	1.56	1.45	1.46	1.43	1.46	1.45	1.46	1.43	1.49	1.62	1.48	1.45	1.70	1.68
Cr	0.02	0.02	0.02	0.03	0.03	0.04	0.03	0.03	0.00	0.03	0.05	0.05	0.03	0.03	0.03	0.04	0.03	0.04
Fe	1.10	1.13	1.15	1.10	1.06	1.05	1.06	1.12	1.08	1.07	1.05	1.07	1.05	1.00	1.00	1.02	1.08	1.08
Mn	0.00	0.00	0.00	0.00	0.00	0.00	0.01	0.00	0.00	0.00	0.00	0.00	0.00	0.01	0.00	0.00	0.00	0.01
Mg	1.10	1.12	1.12	1.12	1.11	1.30	1.32	1.28	1.32	1.32	1.39	1.37	1.52	1.43	1.42	1.43	1.22	1.17
Ca	0.00	0.00	0.00	0.00	0.00	0.00	0.00	0.00	0.00	0.00	0.00	0.00	0.00	0.00	0.00	0.00	0.00	0.00
Na	0.03	0.02	0.02	0.03	0.04	0.03	0.02	0.02	0.03	0.03	0.03	0.02	0.02	0.02	0.03	0.03	0.05	0.04
K	0.89	0.91	0.84	0.86	0.86	0.91	0.95	0.94	0.92	0.92	0.90	0.92	0.87	0.85	0.90	0.91	0.96	0.92
Total	7.69	7.73	7.67	7.67	7.66	7.76	7.80	7.79	7.78	7.78	7.80	7.80	7.84	7.78	7.78	7.80	7.84	7.78
X_{Mg}	0.50	0.50	0.50	0.51	0.51	0.55	0.55	0.53	0.55	0.55	0.57	0.56	0.59	0.59	0.59	0.58	0.53	0.52
X_{Fe}	0.50	0.50	0.50	0.49	0.49	0.45	0.45	0.47	0.45	0.45	0.43	0.44	0.41	0.41	0.41	0.42	0.47	0.48

Table I contd……..

Area	Pavagada					Bidaloti									Bandihalli			
Sample No.	P-18					BID-06		BID-07		BID-09			B-06-07		BHA-07			
Oxides	17	19C	20C	21R	22C	1	10	8	14	3	15	19	14	16	1	5	7	13
SiO_2	36.30	36.62	36.48	35.45	35.83	39.35	37.89	37.32	37.28	35.58	35.69	35.52	37.16	37.99	37.15	37.66	37.73	36.42
TiO_2	4.12	3.78	4.03	4.16	4.51	2.94	3.85	2.44	2.06	3.54	3.49	3.76	2.75	2.74	1.92	1.67	1.58	1.63
Al_2O_3	17.08	17.41	16.91	16.32	17.06	17.24	16.57	18.15	18.28	16.06	16.68	16.16	17.29	17.33	18.24	18.39	18.05	18.00
Cr_2O_3	0.66	0.62	0.65	0.50	0.54	0.04	0.00	0.28	0.45	0.22	0.15	0.23	0.12	0.10	0.06	0.05	0.12	0.00
FeO	17.84	16.69	17.26	17.30	16.79	11.62	12.15	14.95	14.93	15.57	14.42	14.63	11.48	10.94	13.31	12.55	13.50	15.82
MnO	0.09	0.00	0.02	0.13	0.02	0.04	0.05	0.03	0.05	0.05	0.00	0.05	0.04	0.01	0.00	0.02	0.00	0.04
MgO	11.66	11.56	11.44	11.20	11.77	17.87	17.60	14.65	14.78	14.47	14.71	14.79	18.07	18.58	15.46	15.95	14.58	14.01
CaO	0.00	0.00	0.00	0.00	0.02	0.00	0.00	0.00	0.00	0.00	0.01	0.00	0.06	0.00	0.12	0.01	0.00	0.05
Na_2O	0.11	0.23	0.23	0.15	0.17	0.17	0.23	0.08	0.06	0.17	0.27	0.21	0.08	0.26	0.41	0.41	0.43	0.24
K_2O	9.77	9.17	9.71	9.29	9.33	7.68	7.86	7.55	7.90	8.13	8.56	8.99	5.61	6.28	9.10	9.76	9.57	9.12
Total	97.63	96.08	96.74	94.51	96.03	96.93	96.19	95.44	95.78	93.77	93.98	94.33	92.67	94.24	95.77	96.45	95.57	95.33
Cation Numbers based on (O) 11																		
Si	2.69	2.73	2.72	2.71	2.68	2.79	2.73	2.74	2.73	2.70	2.69	2.68	2.74	2.75	2.72	2.74	2.78	2.72
Ti	0.23	0.21	0.23	0.24	0.25	0.16	0.21	0.13	0.11	0.20	0.20	0.21	0.15	0.15	0.11	0.09	0.09	0.09
Al	1.49	1.53	1.49	1.47	1.51	1.44	1.41	1.57	1.58	1.44	1.48	1.44	1.50	1.48	1.58	1.58	1.57	1.58
Cr	0.04	0.04	0.04	0.03	0.03	0.00	0.00	0.02	0.03	0.01	0.01	0.01	0.01	0.01	0.00	0.00	0.01	0.00
Fe	1.11	1.04	1.08	1.11	1.05	0.69	0.73	0.92	0.91	0.99	0.91	0.92	0.71	0.66	0.82	0.76	0.83	0.99
Mn	0.01	0.00	0.00	0.01	0.00	0.00	0.00	0.00	0.00	0.00	0.00	0.00	0.00	0.00	0.00	0.00	0.00	0.00
Mg	1.29	1.28	1.27	1.28	1.31	1.89	1.89	1.60	1.61	1.63	1.65	1.66	1.98	2.00	1.69	1.73	1.60	1.56
Ca	0.00	0.00	0.00	0.00	0.00	0.00	0.00	0.00	0.00	0.00	0.00	0.00	0.00	0.00	0.01	0.00	0.00	0.00
Na	0.02	0.03	0.03	0.02	0.02	0.02	0.03	0.01	0.01	0.02	0.04	0.03	0.01	0.04	0.06	0.06	0.06	0.03
K	0.92	0.87	0.92	0.91	0.89	0.69	0.72	0.71	0.74	0.79	0.82	0.87	0.53	0.58	0.85	0.90	0.90	0.87
Total	7.79	7.73	7.77	7.77	7.75	7.69	7.73	7.69	7.73	7.78	7.80	7.83	7.63	7.67	7.83	7.86	7.83	7.85
X_{Mg}	0.54	0.55	0.54	0.54	0.56	0.73	0.72	0.64	0.64	0.62	0.65	0.64	0.74	0.75	0.67	0.69	0.66	0.61
X_{Fe}	0.46	0.45	0.46	0.46	0.44	0.27	0.28	0.36	0.36	0.38	0.35	0.36	0.26	0.25	0.33	0.31	0.34	0.39

Cordierite: The chemical data of cordierite of all the studied area metapelites are presented in Table II. Mineral formulae were calculated on the basis of 18 (O) atoms. All analyzed cordierite grains have approximately ideal 5.00 Si and 4.00 Al atoms per formula unit (p.f.u). All Fe is calculated as Fe^{+2}. The cation sum is nearly 11.00, indicating only low amount of Fe^{3+}. Na and Ca contents of cordierites are extremely low. The analyzed cordierites are essentially Mg-cordierites and

characteristically their X_{Mg} values (ranging from 0.64-0.79 for Pavagada area, 0.77-0.88 for Bidaloti area and 0.73-0.75 for Bandihalli area) are always more than the associated ferromagnesian minerals, because of the fact that Mg-atoms preferably occupy the octahedral position in the cordierite structure and cordierites with $Fe^{+2} >1$ pfu are rare in nature.

Table. II. Chemical analysis of Cordierite.

Area	Pavagada																	
Sample No.	P-01				P-02				P-10				P-11		P-14		P-16	
Oxides	3	4	5	13	3	7	17	23	2	4	10	27	10	14	4	6	15	17
SiO_2	50.18	49.61	48.99	50.11	54.13	52.26	52.28	53.20	48.20	49.22	45.80	50.12	48.95	50.17	48.15	47.51	48.45	48.30
TiO_2	0.02	0.00	0.00	0.00	0.00	0.00	0.00	0.00	0.00	0.02	0.01	0.00	0.03	0.00	0.02	0.00	0.01	0.00
Al_2O_3	32.76	32.63	33.09	33.37	32.50	31.94	33.18	33.52	33.55	33.04	34.04	32.08	33.26	34.13	34.26	33.63	33.47	33.35
Cr_2O_3	0.00	0.01	0.00	0.00	0.01	0.04	0.01	0.03	0.00	0.00	0.00	0.00	0.00	0.00	0.00	0.01	0.01	0.02
FeO	7.08	7.12	7.14	8.11	4.77	5.29	4.77	5.33	7.70	7.96	7.74	7.12	6.26	6.47	6.64	6.33	7.38	7.70
MnO	0.14	0.14	0.12	0.09	0.01	0.01	0.01	0.00	0.11	0.13	0.15	0.16	0.10	0.13	0.04	0.08	0.13	0.21
MgO	8.06	7.75	8.50	8.12	10.04	8.88	9.64	9.32	9.10	8.85	9.14	9.02	9.80	9.99	10.08	10.22	9.00	8.95
CaO	0.01	0.01	0.02	0.03	0.02	0.02	0.02	0.03	0.01	0.02	0.03	0.03	0.02	0.02	0.01	0.02	0.02	0.02
Na_2O	0.11	0.18	0.16	0.15	0.12	0.10	0.06	0.07	0.13	0.13	0.13	0.15	0.19	0.07	0.11	0.14	0.13	0.18
K_2O	0.00	0.00	0.01	0.00	0.00	0.00	0.00	0.00	0.00	0.00	0.01	0.00	0.01	0.02	0.00	0.00	0.00	0.00
Total	98.34	97.45	98.03	99.98	101.60	98.53	99.97	101.50	98.79	99.36	97.04	98.69	98.63	101.00	99.31	97.93	98.60	98.73
Cation Numbers based on (O) 18																		
Si	5.12	5.11	5.03	5.04	5.27	5.26	5.18	5.20	4.93	5.01	4.79	5.11	4.98	4.98	4.88	4.88	4.96	4.95
Ti	0.00	0.00	0.00	0.00	0.00	0.00	0.00	0.00	0.00	0.00	0.00	0.00	0.00	0.00	0.00	0.00	0.00	0.00
Al	3.94	3.96	4.00	3.96	3.73	3.79	3.88	3.86	4.05	3.96	4.19	3.85	3.99	4.00	4.09	4.07	4.04	4.03
Cr	0.00	0.00	0.00	0.00	0.00	0.00	0.00	0.00	0.00	0.00	0.00	0.00	0.00	0.00	0.00	0.00	0.00	0.00
Fe	0.60	0.61	0.61	0.68	0.39	0.45	0.40	0.44	0.66	0.68	0.68	0.61	0.53	0.54	0.56	0.54	0.63	0.66
Mn	0.01	0.01	0.01	0.01	0.00	0.00	0.00	0.00	0.01	0.01	0.01	0.01	0.01	0.01	0.00	0.01	0.01	0.02
Mg	1.22	1.19	1.30	1.22	1.46	1.33	1.42	1.36	1.39	1.34	1.42	1.37	1.49	1.48	1.52	1.56	1.37	1.37
Ca	0.00	0.00	0.00	0.00	0.00	0.00	0.00	0.00	0.00	0.00	0.00	0.00	0.00	0.00	0.00	0.00	0.00	0.00
Na	0.02	0.03	0.03	0.03	0.02	0.02	0.01	0.01	0.03	0.03	0.03	0.03	0.04	0.01	0.02	0.03	0.03	0.04
K	0.00	0.00	0.00	0.00	0.00	0.00	0.00	0.00	0.00	0.00	0.00	0.00	0.00	0.00	0.00	0.00	0.00	0.00
Total	10.92	10.93	10.99	10.95	10.87	10.85	10.89	10.87	11.06	11.03	11.13	10.98	11.04	11.03	11.08	11.10	11.04	11.06
X_{Mg}	0.67	0.66	0.68	0.64	0.79	0.75	0.78	0.76	0.68	0.66	0.68	0.69	0.74	0.73	0.73	0.74	0.68	0.67
X_{Fe}	0.33	0.34	0.32	0.36	0.21	0.25	0.22	0.24	0.32	0.34	0.32	0.31	0.26	0.27	0.27	0.26	0.32	0.33

Table II contd…..

Area	Pavagada		Bidaloti													Bandihalli		
Sample No.	P-18		BID-06			BID-07			BID-09				B-06-07			BHA-07		
Oxides	6R	7C	8	11	14	5	9	15	17	4	9	16	3	13	17	6	8	9
SiO_2	48.12	48.17	49.84	50.80	49.39	48.82	49.57	48.61	49.83	47.93	47.24	48.34	49.55	49.50	49.31	48.37	49.86	49.41
TiO_2	0.01	0.03	0.01	0.04	0.00	0.01	0.00	0.01	0.00	0.01	0.00	0.00	0.00	0.03	0.00	0.00	0.01	0.00
Al_2O_3	33.52	33.63	33.61	33.58	32.87	31.02	32.56	32.98	32.48	33.15	33.38	33.50	33.53	33.10	33.75	33.37	33.27	32.94
Cr_2O_3	0.02	0.00	0.00	0.02	0.06	0.00	0.05	0.00	0.02	0.00	0.03	0.00	0.00	0.04	0.00	0.00	0.00	0.00
FeO	6.84	6.69	3.11	2.94	2.90	5.42	5.34	5.23	5.19	4.98	4.84	4.84	3.51	3.43	3.29	5.98	5.92	6.34
MnO	0.10	0.07	0.06	0.03	0.03	0.10	0.14	0.13	0.07	0.06	0.14	0.10	0.04	0.07	0.05	0.07	0.02	0.00
MgO	9.24	8.72	11.98	12.12	11.63	10.04	10.30	10.27	10.53	10.71	10.83	10.79	11.49	11.65	11.86	9.60	9.94	9.80
CaO	0.01	0.01	0.02	0.01	0.00	0.03	0.02	0.02	0.00	0.02	0.01	0.02	0.00	0.00	0.02	0.03	0.01	0.01
Na_2O	0.16	0.11	0.27	0.33	0.23	0.21	0.19	0.13	0.19	0.14	0.13	0.17	0.16	0.16	0.18	0.19	0.17	0.13
K_2O	0.00	0.00	0.01	0.01	0.00	0.01	0.01	0.01	0.00	0.01	0.00	0.00	0.00	0.01	0.01	0.00	0.00	0.00
Total	98.00	97.42	98.90	99.87	97.11	95.64	98.17	97.38	98.32	97.02	96.60	97.75	98.29	97.97	98.45	97.60	99.20	98.62
Cation Numbers based on (O) 18																		
Si	4.94	4.97	4.99	5.03	5.02	5.10	5.04	4.99	5.06	4.93	4.89	4.94	4.99	5.00	4.96	4.97	5.03	5.02
Ti	0.00	0.00	0.00	0.00	0.00	0.00	0.00	0.00	0.00	0.00	0.00	0.00	0.00	0.00	0.00	0.00	0.00	0.00
Al	4.06	4.09	3.96	3.92	3.94	3.82	3.91	3.99	3.89	4.02	4.07	4.03	3.98	3.95	4.00	4.04	3.95	3.95
Cr	0.00	0.00	0.00	0.00	0.01	0.00	0.00	0.00	0.00	0.00	0.00	0.00	0.00	0.00	0.00	0.00	0.00	0.00
Fe	0.59	0.58	0.26	0.24	0.25	0.47	0.45	0.45	0.44	0.43	0.42	0.41	0.30	0.29	0.28	0.51	0.50	0.54
Mn	0.01	0.01	0.00	0.00	0.00	0.01	0.01	0.01	0.01	0.00	0.01	0.01	0.00	0.01	0.00	0.01	0.00	0.00
Mg	1.41	1.34	1.79	1.79	1.76	1.56	1.56	1.57	1.59	1.64	1.67	1.64	1.73	1.76	1.78	1.47	1.49	1.48
Ca	0.00	0.00	0.00	0.00	0.00	0.00	0.00	0.00	0.00	0.00	0.00	0.00	0.00	0.00	0.00	0.00	0.00	0.00
Na	0.03	0.02	0.05	0.06	0.04	0.04	0.04	0.03	0.04	0.03	0.03	0.03	0.03	0.03	0.03	0.04	0.03	0.03
K	0.00	0.00	0.00	0.00	0.00	0.00	0.00	0.00	0.00	0.00	0.00	0.00	0.00	0.00	0.00	0.00	0.00	0.00
Total	11.04	11.00	11.06	11.04	11.03	11.01	11.02	11.03	11.02	11.07	11.09	11.07	11.03	11.04	11.06	11.03	11.01	11.02
X_{Mg}	0.71	0.70	0.87	0.88	0.88	0.77	0.77	0.78	0.78	0.79	0.80	0.80	0.85	0.86	0.87	0.74	0.75	0.73
X_{Fe}	0.29	0.30	0.13	0.12	0.12	0.23	0.23	0.22	0.22	0.21	0.20	0.20	0.15	0.14	0.13	0.26	0.25	0.27

The cordierite of Pavagada area (sample No. P-02) was subjected to XRD analysis because of their unusual optical characters and XRD pattern (Fig. 14) corresponded to sub-distortional cordierite with distortion index (Δ) ranges from 0.252 to 0.273. The temperature stability of sub- distortional cordierite is $>900^0$ C. Further, according to Miyashiro (1957) the structural changes and decomposition becomes lower with increasing Fe^{+2}/Mg ratio. The cordierite from Pavagada area has a ratio of 24.40, which confirms its formation at higher temperature close to 900^0C.
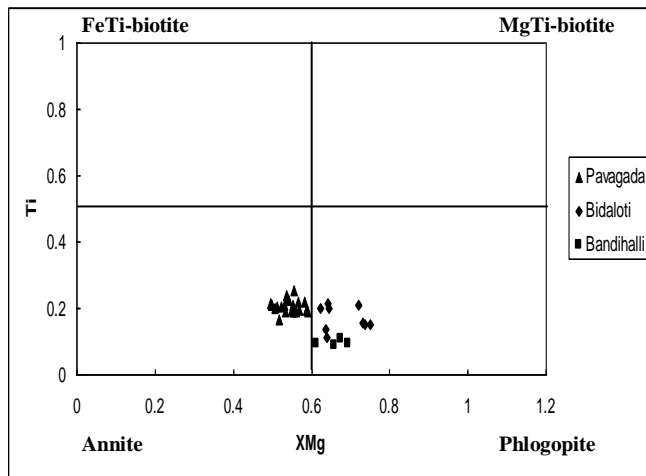

Fig. 13. Plot of X_{Mg} Vs Ti of biotites.
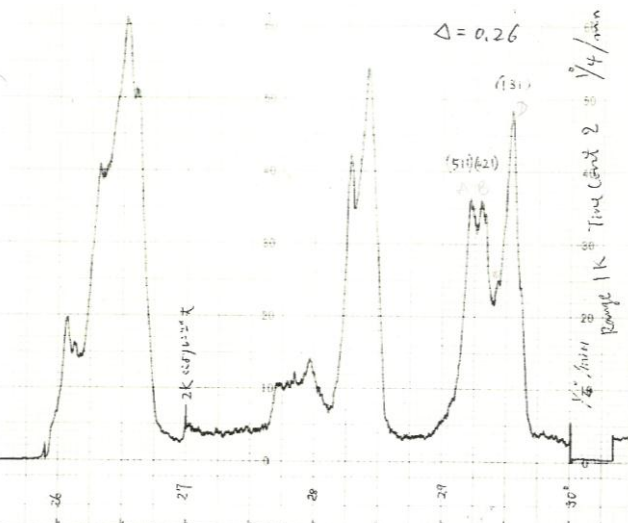
Fig. 14. XRD pattern of Cordierite corresponded to sub-distortional cordierite with a distortion index 0.26.

Garnet: Stochiometric calculations of the garnet of all the studied area metapelites on the basis of 24 (O) atoms give near ideal 6.00 Si and ~4.00 Al pfu is presented in Table III. This suggests the presence of only small amount of Fe^{+3}. Generally, all the studied garnet crystals are almandine-pyrope rich with X_{Fe} values vary from 0.68-0.79 in Pavagada area and 0.70-0.74 in Bandihalli area where as X_{Mg} values vary from 0.19-0.29 in Pavagada area and 0.20-0.24 in Bandihalli area. On (FeO+MgO) Vs (CaO+MnO) diagram (Fig. 15), all the garnet plot in the sillimanite zone.

Table. III. Chemical analysis of Garnet.

Area	Pavagada															Bandihalli		
Sample No.	P-02										P-02A-A		P-02A-B			BHA-07		
Oxides	5C	4R	44C	27R	16C	45C	26R	5'C	14R	1C	8	10	16C	17R	28	2C	3M	4R
SiO_2	43.36	36.96	40.37	39.77	40.85	40.29	39.71	40.77	41.31	37.79	38.27	38.14	38.11	37.26	38.42	38.18	39.03	38.39
TiO_2	0.02	0.02	0.01	0.03	0.00	0.01	0.01	0.02	0.08	0.01	0.01	0.04	0.01	0.02	0.02	0.02	0.02	0.03
Al_2O_3	20.83	20.03	21.71	21.58	22.04	21.34	20.05	21.01	21.05	20.85	20.35	20.95	20.07	21.14	20.72	21.32	21.49	21.13
Cr_2O_3	0.00	0.03	0.05	0.02	0.04	0.08	0.01	0.00	0.02	0.02	0.12	0.35	0.11	0.14	0.25	0.05	0.05	0.00
FeO	30.64	31.90	31.56	33.35	33.95	32.69	32.20	30.97	35.64	30.72	33.69	32.67	31.82	31.78	32.65	32.71	32.31	34.38
MnO	0.24	0.24	0.22	0.30	0.27	0.24	0.26	0.25	0.32	0.13	0.18	0.16	0.29	0.20	0.29	0.89	0.89	1.00
MgO	7.25	5.88	6.49	5.84	5.98	6.42	5.77	6.60	4.92	5.79	6.79	7.32	6.94	7.65	7.57	6.26	6.33	5.14
CaO	1.17	0.46	0.97	0.58	0.61	1.13	0.58	1.13	0.43	0.69	0.91	0.83	1.01	0.92	0.76	1.45	1.48	1.62
Na_2O	0.01	0.01	0.01	0.00	0.00	0.00	0.00	0.00	0.00	0.00	0.00	0.00	0.00	0.01	0.00	0.00	0.01	0.00
K_2O	0.00	0.01	0.00	0.01	0.00	0.00	0.00	0.00	0.00	0.00	0.00	0.01	0.00	0.00	0.00	0.00	0.00	0.01
Total	103.52	95.54	101.40	101.48	103.74	102.19	98.60	100.75	103.77	95.99	100.31	100.47	98.36	99.11	100.68	100.88	101.61	101.69
Cation Numbers based on (O) 24																		
Si	6.44	6.09	6.19	6.15	6.17	6.17	6.30	6.28	6.28	6.14	6.04	5.98	6.09	5.91	6.01	5.98	6.04	6.01
Ti	0.00	0.00	0.00	0.00	0.00	0.00	0.00	0.00	0.01	0.00	0.00	0.00	0.00	0.00	0.00	0.00	0.00	0.00
Al	3.65	3.89	3.92	3.93	3.92	3.85	3.75	3.81	3.77	4.00	3.79	3.87	3.78	3.95	3.82	3.94	3.92	3.90
Cr	0.00	0.00	0.01	0.00	0.00	0.01	0.00	0.00	0.00	0.00	0.01	0.04	0.01	0.02	0.03	0.01	0.01	0.00
Fe	3.81	4.40	4.05	4.31	4.29	4.19	4.27	3.99	4.53	4.18	4.45	4.28	4.25	4.22	4.27	4.29	4.18	4.50
Mn	0.03	0.03	0.03	0.04	0.03	0.03	0.04	0.03	0.04	0.02	0.02	0.02	0.04	0.03	0.04	0.12	0.12	0.13
Mg	1.61	1.44	1.48	1.34	1.35	1.46	1.36	1.51	1.11	1.40	1.60	1.71	1.65	1.81	1.76	1.46	1.46	1.20
Ca	0.19	0.08	0.16	0.10	0.10	0.19	0.10	0.19	0.07	0.12	0.15	0.14	0.17	0.16	0.13	0.24	0.25	0.27
Na	0.00	0.00	0.00	0.00	0.00	0.00	0.00	0.00	0.00	0.00	0.00	0.00	0.00	0.00	0.00	0.00	0.00	0.00
K	0.00	0.00	0.00	0.00	0.00	0.00	0.00	0.00	0.00	0.00	0.00	0.00	0.00	0.00	0.00	0.00	0.00	0.00
Total	15.73	15.96	15.84	15.88	15.87	15.90	15.82	15.81	15.82	15.86	16.06	16.06	16.01	16.10	16.06	16.04	15.99	16.03
X_{Fe}	0.68	0.74	0.71	0.74	0.74	0.71	0.74	0.70	0.79	0.73	0.71	0.70	0.70	0.68	0.69	0.70	0.70	0.74
X_{Mn}	0.01	0.01	0.01	0.01	0.01	0.01	0.01	0.01	0.01	0.00	0.00	0.00	0.01	0.00	0.01	0.02	0.02	0.02
X_{Mg}	0.29	0.24	0.26	0.23	0.23	0.25	0.24	0.26	0.19	0.25	0.26	0.28	0.27	0.29	0.28	0.24	0.24	0.20
X_{Ca}	0.03	0.01	0.03	0.02	0.02	0.03	0.02	0.03	0.01	0.02	0.02	0.02	0.03	0.03	0.02	0.04	0.04	0.04

Orthoamphibole: The chemistry of orthoamphiboles of all the studied area metapelites are presented in Table IV. The cations are calculated on the basis of 23 (O) atoms and their sums are found to be around 15.00. Orthoamphibole is generally characterized by low MnO, CaO and Na_2O. However notable quantity of CaO and Na_2O are seen in some analyses. The orthoamphiboles of Pavagada and Bidaloti area compositionally correspond to Mg-anthophyllite whereas Bandihalli area correspond to gedrite as inferred from Leake's (1978) diagram (Fig. 16).

Table. IV. Chemical analysis of Orthoamphibole.

Area	Pavagada														Bidaloti			
Sample No.	P-02A-A			P-10			P-11			P-14			P-18		BID-06			
Oxides	2	5	20	32R	33C	36	3	8	19	3	15	21	10R	11C	2	4	5	6
SiO_2	50.05	48.48	51.61	53.60	53.27	54.33	55.49	53.23	53.67	49.94	51.98	49.12	51.35	50.40	54.89	55.25	55.20	54.13
TiO_2	0.09	0.10	0.04	0.12	0.06	0.09	0.11	0.09	0.05	0.05	0.07	0.00	0.15	0.16	0.15	0.13	0.13	0.14
Al_2O_3	5.02	4.51	2.09	2.62	2.34	2.78	2.87	2.35	2.20	2.52	3.39	13.31	3.31	3.64	2.12	2.16	2.36	2.22
Cr_2O_3	0.19	0.61	0.13	0.13	0.00	0.00	0.21	0.28	0.22	0.30	0.27	0.10	0.12	0.22	0.07	0.01	0.03	0.01
FeO	24.48	24.71	23.19	24.61	25.03	25.38	22.20	23.32	25.70	24.37	24.45	19.81	24.98	24.78	15.80	15.87	15.93	15.86
MnO	0.11	0.14	0.07	0.39	0.46	0.44	0.50	0.35	0.51	0.38	0.35	0.32	0.38	0.36	0.32	0.28	0.19	0.18
MgO	16.17	16.55	18.59	15.19	16.33	15.92	15.23	16.90	16.02	17.31	17.10	11.30	15.64	15.37	23.52	22.94	23.39	23.42
CaO	0.06	0.07	0.06	0.15	0.12	0.13	0.17	0.18	0.14	0.13	0.18	4.78	0.23	0.24	0.21	0.25	0.16	0.15
Na_2O	0.29	0.33	0.06	0.20	0.13	0.17	0.19	0.11	0.15	0.10	0.22	0.42	0.21	0.22	0.21	0.19	0.15	0.12
K_2O	0.00	0.00	0.01	0.00	0.01	0.01	0.01	0.00	0.02	0.00	0.00	0.02	0.01	0.00	0.01	0.02	0.01	0.00
Total	96.45	95.49	95.83	96.99	97.75	99.24	96.97	96.80	98.67	95.10	98.00	99.16	96.39	95.38	97.30	97.10	97.55	96.24
Cation Numbers based on (O) 23																		
Si	7.46	7.35	7.69	7.90	7.82	7.84	8.05	7.83	7.83	7.58	7.61	7.01	7.67	7.62	7.75	7.81	7.77	7.73
Ti	0.01	0.01	0.00	0.01	0.01	0.01	0.01	0.01	0.01	0.01	0.01	0.00	0.02	0.02	0.02	0.01	0.01	0.02
Al	0.88	0.81	0.37	0.46	0.40	0.47	0.49	0.41	0.38	0.45	0.59	2.24	0.58	0.65	0.35	0.36	0.39	0.37
Cr	0.02	0.07	0.01	0.02	0.00	0.00	0.02	0.03	0.03	0.04	0.03	0.01	0.01	0.03	0.01	0.00	0.00	0.00
Fe	3.05	3.13	2.89	3.03	3.07	3.06	2.69	2.87	3.14	3.09	3.00	2.36	3.12	3.13	1.87	1.88	1.87	1.89
Mn	0.01	0.02	0.01	0.05	0.06	0.05	0.06	0.04	0.06	0.05	0.04	0.04	0.05	0.05	0.04	0.03	0.02	0.02
Mg	3.59	3.74	4.13	3.34	3.57	3.42	3.29	3.71	3.48	3.92	3.73	2.40	3.48	3.46	4.95	4.83	4.90	4.99
Ca	0.01	0.01	0.01	0.02	0.02	0.02	0.03	0.03	0.02	0.02	0.03	0.73	0.04	0.04	0.03	0.04	0.02	0.02
Na	0.08	0.10	0.02	0.06	0.04	0.05	0.05	0.03	0.04	0.03	0.06	0.12	0.06	0.06	0.06	0.05	0.04	0.03
K	0.00	0.00	0.00	0.00	0.00	0.00	0.00	0.00	0.00	0.00	0.00	0.00	0.00	0.00	0.00	0.00	0.00	0.00
Total	15.12	15.24	15.13	14.88	14.99	14.94	14.71	14.96	14.99	15.18	15.10	14.92	15.04	15.06	15.08	15.02	15.04	15.08
X_{Mg}	0.54	0.54	0.59	0.52	0.54	0.53	0.55	0.56	0.53	0.56	0.55	0.50	0.53	0.53	0.73	0.72	0.72	0.72
X_{Fe}	0.46	0.46	0.41	0.48	0.46	0.47	0.45	0.44	0.47	0.44	0.45	0.50	0.47	0.47	0.27	0.28	0.28	0.28

Table. IV contd…………..

Area	Bidaloti															Bandihalli		
Sample No.	BID-06			BID-07				BID-09					B-06-07			BHA-07		
Oxides	9	12	13	1	4	7	16	1	3	7	8	10	6	12	19	10	11	12
SiO_2	54.50	55.05	55.54	53.02	52.06	50.67	53.98	54.53	53.53	54.42	54.24	55.23	52.84	54.14	53.37	45.34	46.69	46.50
TiO_2	0.07	0.18	0.17	0.06	0.13	0.11	0.09	0.12	0.21	0.14	0.10	0.09	0.18	0.06	0.15	0.23	0.21	0.24
Al_2O_3	1.84	2.40	2.19	3.17	3.63	4.45	2.87	2.39	2.96	2.44	2.11	2.08	3.54	1.44	2.61	12.75	11.12	12.41
Cr_2O_3	0.00	0.00	0.03	0.15	0.27	0.11	0.10	0.04	0.00	0.04	0.00	0.05	0.05	0.02	0.01	0.04	0.01	0.00
FeO	15.59	16.12	15.93	21.46	21.96	21.85	21.57	16.04	15.96	15.93	16.41	15.68	16.75	16.64	17.18	24.00	24.04	23.93
MnO	0.26	0.30	0.22	0.36	0.38	0.37	0.34	0.30	0.32	0.30	0.30	0.28	0.43	0.25	0.41	0.25	0.26	0.19
MgO	24.01	23.19	23.26	18.77	18.23	18.45	18.65	23.43	23.08	23.12	22.62	23.27	22.12	23.13	22.41	12.96	13.74	13.67
CaO	0.17	0.21	0.21	0.18	0.29	0.27	0.17	0.20	0.21	0.18	0.19	0.18	0.29	0.20	0.25	0.43	0.41	0.39
Na_2O	0.14	0.20	0.15	0.23	0.34	0.27	0.25	0.19	0.31	0.17	0.17	0.11	0.39	0.06	0.23	1.09	1.14	1.11
K_2O	0.00	0.01	0.00	0.02	0.00	0.02	0.00	0.00	0.00	0.01	0.01	0.00	0.00	0.00	0.00	0.01	0.00	0.01
Total	96.57	97.66	97.70	97.43	97.28	96.55	98.02	97.23	96.58	96.75	96.14	96.97	96.59	95.95	96.63	97.08	97.62	98.44
Cation Numbers based on (O) 23																		
Si	7.75	7.75	7.80	7.69	7.60	7.46	7.77	7.72	7.64	7.74	7.78	7.81	7.58	7.79	7.66	6.74	6.90	6.80
Ti	0.01	0.02	0.02	0.01	0.01	0.01	0.01	0.01	0.02	0.01	0.01	0.01	0.02	0.01	0.02	0.03	0.02	0.03
Al	0.31	0.40	0.36	0.54	0.62	0.77	0.49	0.40	0.50	0.41	0.36	0.35	0.60	0.24	0.44	2.23	1.94	2.14
Cr	0.00	0.00	0.00	0.02	0.03	0.01	0.01	0.00	0.00	0.00	0.00	0.01	0.01	0.00	0.00	0.00	0.00	0.00
Fe	1.85	1.90	1.87	2.60	2.68	2.69	2.60	1.90	1.91	1.89	1.97	1.85	2.01	2.00	2.06	2.98	2.97	2.93
Mn	0.03	0.04	0.03	0.04	0.05	0.05	0.04	0.04	0.04	0.04	0.04	0.03	0.05	0.03	0.05	0.03	0.03	0.02
Mg	5.09	4.87	4.87	4.06	3.97	4.05	4.00	4.94	4.91	4.90	4.83	4.90	4.73	4.96	4.79	2.87	3.03	2.98
Ca	0.03	0.03	0.03	0.03	0.05	0.04	0.03	0.03	0.03	0.03	0.03	0.03	0.04	0.03	0.04	0.07	0.06	0.06
Na	0.04	0.05	0.04	0.07	0.10	0.08	0.07	0.05	0.08	0.05	0.05	0.03	0.11	0.02	0.06	0.31	0.33	0.32
K	0.00	0.00	0.00	0.00	0.00	0.00	0.00	0.00	0.00	0.00	0.00	0.00	0.00	0.00	0.00	0.00	0.00	0.00
Total	15.11	15.06	15.02	15.06	15.11	15.17	15.01	15.09	15.13	15.07	15.06	15.02	15.15	15.09	15.13	15.27	15.28	15.27
X_{Mg}	0.73	0.72	0.72	0.61	0.60	0.60	0.61	0.72	0.72	0.72	0.71	0.73	0.70	0.71	0.70	0.49	0.50	0.50
X_{Fe}	0.27	0.28	0.28	0.39	0.40	0.40	0.39	0.28	0.28	0.28	0.29	0.27	0.30	0.29	0.30	0.51	0.50	0.50

Orthopyroxene: The chemical analyses of orthopyroxene of all the studied metapelites are presented in Table V along with the structural formula based on 6 (O) atoms. The sum of cations is nearly equal to 4.00 indicating low Fe^{+3} in Opx. The Al_2O_3 content of Opx varies from 2.7 to 6.9 wt% in Pavagada area and 2.21 to 3.36 wt% in Bidaloti area. Whereas the X_{Mg} value varies from 0.51 to 0.61 in Pavagada area and 0.56 to 0.72 in Bidaloti area. Overall the studied orthopyroxenes corresponds to hypersthene (See Fig. 17).

Table. V. Chemical analysis of Orthopyroxene.

Area	Pavagada																	
Sample No.	P-02					P-02A-A		P-02A-B		P-11				P-14				
Oxides	8C	9R	22C	21R	36R	1	4	21R	22C	1C	6	7	22R	1R	2C	4R	14C	22C
SiO_2	51.87	54.55	52.92	57.45	50.08	47.11	47.03	48.03	47.18	50.42	50.84	48.75	49.97	48.70	50.91	48.85	48.85	49.45
TiO_2	0.07	0.07	0.09	0.07	0.03	0.06	0.11	0.10	0.08	0.08	0.06	0.05	0.05	0.04	0.07	0.05	0.05	0.04
Al_2O_3	5.39	4.09	5.53	2.80	6.93	6.49	6.36	6.10	6.19	3.02	2.88	2.89	2.73	2.80	2.86	2.79	2.97	3.17
Cr_2O_3	0.01	0.04	0.04	0.07	0.00	0.11	0.11	0.12	0.12	0.29	0.37	0.36	0.22	0.17	0.25	0.21	0.27	0.14
FeO	27.67	21.78	26.88	21.67	27.94	27.29	26.87	26.74	26.47	28.25	29.20	28.29	28.45	29.22	29.30	28.76	28.23	29.11
MnO	0.11	0.08	0.08	0.03	0.15	0.08	0.15	0.08	0.07	0.54	0.49	0.52	0.48	0.33	0.44	0.45	0.46	0.40
MgO	17.61	17.64	16.62	18.99	16.31	17.53	17.75	17.90	18.28	17.91	17.51	16.41	17.37	18.11	18.12	17.12	17.51	18.71
CaO	0.11	0.07	0.12	0.08	0.05	0.04	0.02	0.04	0.08	0.12	0.14	0.13	0.10	0.09	0.07	0.09	0.09	0.09
Na_2O	0.01	0.35	0.00	0.09	0.01	0.00	0.00	0.00	0.00	0.03	0.05	0.02	0.02	0.02	0.03	0.03	0.02	0.00
K_2O	0.01	0.01	0.01	0.01	0.00	0.00	0.00	0.01	0.00	0.00	0.01	0.01	0.01	0.00	0.01	0.00	0.00	0.00
Total	102.86	98.67	102.28	101.26	101.49	98.70	98.39	99.11	98.47	100.67	101.53	97.43	99.39	99.48	102.05	98.35	98.46	101.11
Cation Numbers based on (O) 6																		
Si	1.91	2.03	1.94	2.07	1.87	1.82	1.82	1.84	1.83	1.92	1.93	1.93	1.93	1.89	1.92	1.92	1.91	1.88
Ti	0.00	0.00	0.00	0.00	0.00	0.00	0.00	0.00	0.00	0.00	0.00	0.00	0.00	0.00	0.00	0.00	0.00	0.00
Al	0.23	0.18	0.24	0.12	0.31	0.30	0.29	0.28	0.28	0.14	0.13	0.13	0.12	0.13	0.13	0.13	0.14	0.14
Cr	0.00	0.00	0.00	0.00	0.00	0.00	0.00	0.00	0.00	0.01	0.01	0.01	0.01	0.01	0.01	0.01	0.01	0.00
Fe	0.85	0.68	0.83	0.65	0.87	0.88	0.87	0.86	0.86	0.90	0.92	0.93	0.92	0.95	0.92	0.94	0.92	0.93
Mn	0.00	0.00	0.00	0.00	0.00	0.00	0.00	0.00	0.00	0.02	0.02	0.02	0.02	0.01	0.01	0.02	0.02	0.01
Mg	0.97	0.98	0.91	1.02	0.91	1.01	1.03	1.02	1.05	1.02	0.99	0.97	1.00	1.05	1.02	1.00	1.02	1.06
Ca	0.00	0.00	0.00	0.00	0.00	0.00	0.00	0.00	0.00	0.00	0.01	0.01	0.00	0.00	0.00	0.00	0.00	0.00
Na	0.00	0.03	0.00	0.01	0.00	0.00	0.00	0.00	0.00	0.00	0.00	0.00	0.00	0.00	0.00	0.00	0.00	0.00
K	0.00	0.00	0.00	0.00	0.00	0.00	0.00	0.00	0.00	0.00	0.00	0.00	0.00	0.00	0.00	0.00	0.00	0.00
Total	3.97	3.89	3.93	3.87	3.97	4.02	4.03	4.01	4.03	4.01	4.01	4.00	4.00	4.04	4.01	4.02	4.02	4.04
X_{Mg}	0.53	0.59	0.52	0.61	0.51	0.53	0.54	0.54	0.55	0.53	0.52	0.51	0.52	0.52	0.52	0.51	0.53	0.53
X_{Fe}	0.47	0.41	0.48	0.39	0.49	0.47	0.46	0.46	0.45	0.47	0.48	0.49	0.48	0.48	0.48	0.49	0.47	0.47

Table. V. Continue……………..

| Area	Bidaloti																	
Sample No.	BID-06		BID-07					BID-09							B-06-07			
Oxides	3	7	2	3	6	11	12	5	6	7	10	13	17	18	1	4	9R	10R
SiO_2	54.36	55.91	51.17	51.36	51.05	50.13	50.24	45.09	48.89	49.78	48.42	49.02	51.07	49.09	52.77	52.07	52.35	51.97
TiO_2	0.07	0.21	0.07	0.11	0.07	0.11	0.05	0.07	0.06	0.07	0.05	0.04	0.07	0.05	0.09	0.06	0.07	0.09
Al_2O_3	2.24	2.55	2.96	3.36	3.30	3.21	3.31	2.63	2.77	2.66	2.73	3.07	2.53	2.76	2.22	2.29	2.41	2.47
Cr_2O_3	0.02	0.02	0.17	0.25	0.28	0.18	0.29	0.06	0.09	0.12	0.01	0.03	0.08	0.01	0.07	0.00	0.00	0.03
FeO	19.05	16.10	26.47	26.33	26.43	26.25	26.98	24.66	24.69	23.73	24.51	24.62	24.42	24.54	20.21	19.78	20.36	20.25
MnO	0.32	0.28	0.44	0.34	0.39	0.42	0.50	0.39	0.40	0.38	0.34	0.33	0.35	0.49	0.43	0.38	0.26	0.44
MgO	25.49	23.58	18.99	18.83	19.48	19.54	19.12	17.74	19.94	20.82	20.25	20.35	20.82	20.59	24.13	23.77	23.99	24.24
CaO	0.08	0.25	0.12	0.15	0.10	0.16	0.10	0.16	0.14	0.15	0.12	0.15	0.14	0.33	0.09	0.10	0.08	0.11
Na_2O	0.00	0.20	0.00	0.00	0.00	0.00	0.00	0.04	0.00	0.02	0.00	0.02	0.01	0.02	0.00	0.01	0.01	0.00
K_2O	0.01	0.01	0.00	0.00	0.00	0.00	0.01	0.04	0.00	0.00	0.01	0.00	0.01	0.01	0.00	0.00	0.00	0.01
Total	101.63	99.11	100.38	100.74	101.10	100.00	100.61	90.88	96.98	97.72	96.41	97.63	99.49	97.88	100.00	98.47	99.52	99.60
Cation Numbers based on (O) 6																		
Si	1.95	2.02	1.93	1.93	1.91	1.90	1.90	1.90	1.91	1.92	1.90	1.90	1.93	1.90	1.94	1.94	1.94	1.92
Ti	0.00	0.01	0.00	0.00	0.00	0.00	0.00	0.00	0.00	0.00	0.00	0.00	0.00	0.00	0.00	0.00	0.00	0.00
Al	0.09	0.11	0.13	0.15	0.15	0.14	0.15	0.13	0.13	0.12	0.13	0.14	0.11	0.13	0.10	0.10	0.10	0.11
Cr	0.00	0.00	0.01	0.01	0.01	0.01	0.01	0.00	0.00	0.00	0.00	0.00	0.00	0.00	0.00	0.00	0.00	0.00
Fe	0.57	0.49	0.84	0.83	0.83	0.83	0.86	0.87	0.81	0.76	0.80	0.80	0.77	0.79	0.62	0.62	0.63	0.63
Mn	0.01	0.01	0.01	0.01	0.01	0.01	0.02	0.01	0.01	0.01	0.01	0.01	0.01	0.02	0.01	0.01	0.01	0.01
Mg	1.36	1.27	1.07	1.05	1.09	1.11	1.08	1.11	1.16	1.19	1.18	1.17	1.17	1.19	1.32	1.32	1.32	1.34
Ca	0.00	0.01	0.00	0.01	0.00	0.01	0.00	0.01	0.01	0.01	0.00	0.01	0.01	0.01	0.00	0.00	0.00	0.00
Na	0.00	0.01	0.00	0.00	0.00	0.00	0.00	0.00	0.00	0.00	0.00	0.00	0.00	0.00	0.00	0.00	0.00	0.00
K	0.00	0.00	0.00	0.00	0.00	0.00	0.00	0.00	0.00	0.00	0.00	0.00	0.00	0.00	0.00	0.00	0.00	0.00
Total	4.00	3.93	4.00	3.99	4.01	4.02	4.02	4.04	4.02	4.02	4.03	4.03	4.01	4.04	4.01	4.00	4.01	4.02
X_{Mg}	0.70	0.72	0.56	0.56	0.57	0.57	0.56	0.56	0.59	0.61	0.60	0.60	0.60	0.60	0.68	0.68	0.68	0.68
X_{Fe}	0.30	0.28	0.44	0.44	0.43	0.43	0.44	0.44	0.41	0.39	0.40	0.40	0.40	0.40	0.32	0.32	0.32	0.32
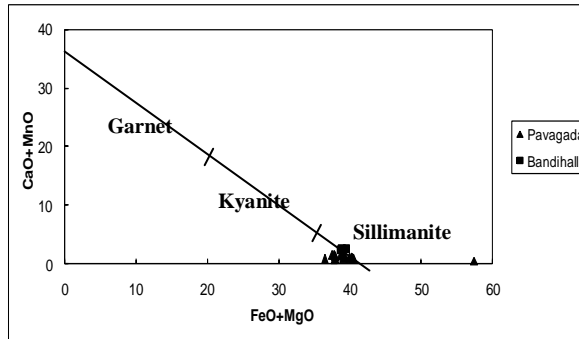
Fig. 15. Nature of variation of (FeO+MgO) with (CaO+MnO) in garnets (after Sturt, 1962).
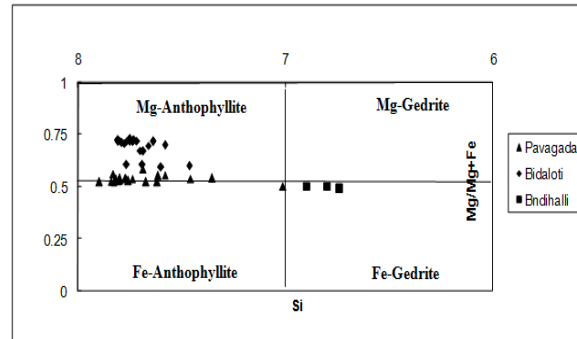

Fig. 16. Compositions of Orthoamphiboles (after Leake, 1978).
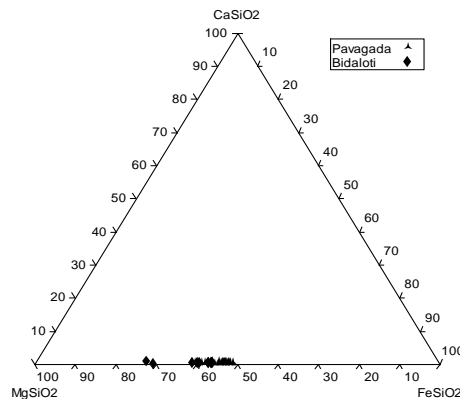

Fig. 17. Nomenclature of orthopyroxenes.
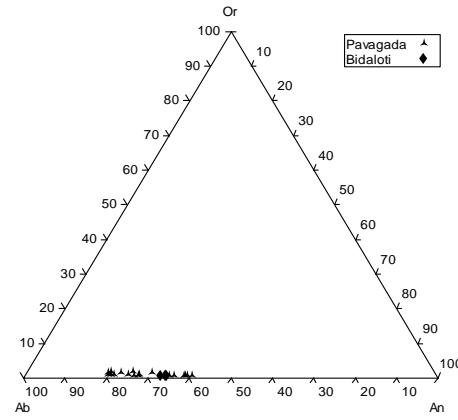
Fig. 18. Feldspar triangle.

Plagioclase: The chemical analyses of Plagioclase of all the studied area metapelites are given in Table VI along with the structural formula based on 8 (O) atoms. The K contents are generally low, varies from 0.003 to 0.015 p.f.u. in Pavagada area and 0.013 to 0.020 p.f.u. in Bidaloti area. All plagioclase compositions are plotted on the feldspar triangle (Fig. 18) corresponds to andesine to oligoclase (%Ab 64.20 to 78.83) in composition for Pavagada area and andesine (%Ab 65.10 to 66.49) in composition for Bidaloti area.

Table. VI. Chemical analysis of Plagioclase.

Area	Pavagada														Bidaloti		
Sample No.	P-11			P-14			P-16								B-06-07		
Oxides	15C	16R	26C	11R	12C	25	1R	2C	3	3'	4C	5R	9C	21C	2	7	8
SiO₂	59.240	59.757	58.378	58.103	58.517	57.359	61.252	61.914	60.702	62.352	64.071	63.115	59.778	60.783	59.306	58.418	59.380
TiO₂	0.017	0.000	0.000	0.000	0.000	0.019	0.014	0.006	0.000	0.007	0.000	0.000	0.026	0.000	0.000	0.022	0.000
Al₂O₃	26.043	25.669	25.533	26.072	25.910	24.229	22.736	21.155	22.610	23.765	23.084	22.182	23.851	23.906	25.002	25.669	25.465
Cr₂O₃	0.029	0.009	0.009	0.000	0.019	0.094	0.000	0.047	0.000	0.000	0.010	0.000	0.011	0.015	0.000	0.000	0.012
FeO	0.000	0.092	0.043	0.013	0.007	0.146	0.027	0.100	0.022	0.000	0.021	0.143	0.043	0.012	0.085	0.000	0.061
MnO	0.000	0.004	0.016	0.015	0.000	0.015	0.023	0.000	0.052	0.034	0.040	0.000	0.016	0.000	0.000	0.046	0.012
MgO	0.021	0.003	0.007	0.006	0.000	0.038	0.009	0.016	0.000	0.008	0.000	0.000	0.000	0.008	0.000	0.017	0.005
CaO	7.130	7.089	7.377	5.536	6.103	5.663	4.764	4.447	4.373	4.467	4.199	4.141	5.116	6.530	7.212	7.225	7.217
Na₂O	7.494	7.536	7.397	8.253	8.551	8.729	9.309	9.183	8.985	9.073	8.960	8.810	9.268	7.981	7.525	7.548	8.028
K₂O	0.087	0.062	0.072	0.054	0.119	0.259	0.126	0.257	0.137	0.088	0.191	0.118	0.226	0.204	0.058	0.082	0.087
Total	100.061	100.221	98.832	98.052	99.226	96.551	98.260	97.125	96.881	99.794	100.576	98.509	98.335	99.439	99.188	99.027	100.267
Cation Numbers based on (O) 8																	
Si	2.639	2.657	2.637	2.636	2.633	2.659	2.769	2.826	2.776	2.765	2.811	2.827	2.710	2.720	10.664	10.535	10.589
Ti	0.001	0.000	0.000	0.000	0.000	0.001	0.000	0.000	0.000	0.000	0.000	0.000	0.001	0.000	0.000	0.003	0.000
Al	1.368	1.345	1.360	1.395	1.375	1.324	1.212	1.139	1.219	1.242	1.194	1.171	1.275	1.261	5.300	5.458	5.354
Cr	0.001	0.000	0.000	0.000	0.001	0.003	0.000	0.002	0.000	0.000	0.000	0.000	0.000	0.001	0.000	0.000	0.002
Fe	0.000	0.003	0.002	0.000	0.000	0.006	0.001	0.004	0.001	0.000	0.001	0.005	0.002	0.000	0.013	0.000	0.009
Mn	0.000	0.000	0.001	0.001	0.000	0.001	0.001	0.000	0.002	0.001	0.001	0.000	0.001	0.000	0.000	0.007	0.002
Mg	0.001	0.000	0.000	0.000	0.000	0.003	0.001	0.001	0.000	0.001	0.000	0.000	0.000	0.001	0.000	0.005	0.001
Ca	0.340	0.338	0.357	0.269	0.294	0.281	0.231	0.218	0.214	0.212	0.197	0.199	0.249	0.313	1.390	1.396	1.379
Na	0.647	0.650	0.648	0.726	0.746	0.785	0.816	0.813	0.797	0.780	0.762	0.765	0.815	0.693	2.624	2.639	2.776
K	0.005	0.004	0.004	0.003	0.007	0.015	0.007	0.015	0.008	0.005	0.011	0.007	0.013	0.012	0.013	0.019	0.020
Total	5.002	4.997	5.009	5.031	5.056	5.077	5.037	5.017	5.017	5.006	4.978	4.974	5.065	5.001	20.004	20.062	20.131
%An	34.288	34.082	35.385	26.959	28.101	26.016	21.894	20.809	21.029	21.282	20.344	20.476	23.091	30.780	34.511	34.436	33.033
%Ab	65.214	65.563	64.204	72.727	71.247	72.567	77.416	77.759	78.186	78.219	78.554	78.829	75.695	68.075	65.159	65.099	66.493
%Or	0.498	0.355	0.411	0.313	0.652	1.417	0.689	1.432	0.784	0.499	1.102	0.695	1.215	1.145	0.330	0.465	0.474

Sillimanite: Sillimanite is the dominant Al-silicate in the metapelitic rocks of the amphibolite facies domain (Dietvorst, 1981) as well as of the granulite facies domain. The chemical analyses of sillimanite of Pavagada area are given in Table VII along with the structural formula based on 5 (O) atoms. These sillimanites generally contain appreciable amount of Cr_2O_3 and FeO. The Al_2O_3 content of studied sillimanite varies from 56.5 to 62.9 wt%.

Table. VII. Chemical analysis of Sillimanite.

Area	Pavagada							
Sample No.	P-01		P-15			P-16		
Oxides	1	18	1	3	1	5	10C	13
SiO_2	38.882	38.083	37.704	35.923	35.812	37.735	34.058	34.280
TiO_2	0.014	0.026	0.000	0.000	0.002	0.000	0.000	0.000
Al_2O_3	60.390	56.552	62.712	62.943	60.494	61.307	62.420	64.140
Cr_2O_3	0.071	0.086	0.000	0.000	0.069	0.003	0.089	0.021
FeO	0.195	0.143	0.218	0.187	0.089	0.199	0.183	0.359
MnO	0.018	0.063	0.044	0.000	0.012	0.000	0.000	0.031
MgO	0.008	0.006	0.019	0.029	0.006	0.000	0.005	0.025
CaO	0.000	0.000	0.014	0.023	0.005	0.000	0.001	0.003
Na_2O	0.000	0.000	0.005	0.006	0.025	0.016	0.033	0.010
K_2O	0.011	0.008	0.016	0.012	0.004	0.020	0.015	0.000
Total	99.589	94.967	100.732	99.123	96.518	99.280	96.804	98.869
Cation Numbers based on (O) 5								
Si	1.052	1.079	4.041	3.918	4.006	4.100	3.809	3.759
Ti	0.000	0.001	0.000	0.000	0.000	0.000	0.000	0.000
Al	1.926	1.889	7.925	8.093	7.977	7.853	8.231	8.292
Cr	0.002	0.002	0.000	0.000	0.006	0.000	0.008	0.002
Fe	0.004	0.003	0.020	0.017	0.008	0.018	0.017	0.033
Mn	0.000	0.002	0.004	0.000	0.001	0.000	0.000	0.003
Mg	0.000	0.000	0.003	0.005	0.001	0.000	0.001	0.004
Ca	0.000	0.000	0.002	0.003	0.001	0.000	0.000	0.000
Na	0.000	0.000	0.001	0.001	0.005	0.003	0.007	0.002
K	0.000	0.000	0.002	0.002	0.001	0.003	0.002	0.000
Total	2.985	2.975	11.998	12.038	12.006	11.977	12.076	12.095

Table. VIII. Chemical analysis of Spinel.

Area	Pavagada																
Sample No.	P-01								P-02	P-02A-A		P-10			P-15		
Oxides	2	6	8	21	22	24	25	28	6	12	14	14	16	17	3	4	7
SiO_2	0.018	0.022	0.051	0.050	0.051	0.026	0.016	0.090	0.037	0.056	0.117	0.013	0.015	0.019	0.01	0.027	0.055
TiO_2	0.031	0.018	0.015	0.000	0.057	0.010	0.004	0.014	0.015	0.02	0.035	0.045	0.003	0.028	0.06	0.033	0.021
Al_2O_3	59.526	57.501	57.803	60.614	61.295	61.442	58.540	57.225	58.692	55.041	57.017	58.326	58.569	57.726	58.291	59.49	58.877
Cr_2O_3	0.379	0.376	0.293	0.164	0.124	0.082	0.247	0.245	0.010	0.157	0.283	0.414	0.147	0.305	0.268	0.153	0.195
FeO	33.421	33.466	33.648	36.089	37.009	34.990	35.643	36.411	32.957	33.695	35.082	35.498	34.987	35.554	34.619	34.271	35.487
MnO	0.237	0.181	0.209	0.255	0.263	0.177	0.186	0.197	0.000	0.073	0.027	0.186	0.195	0.187	0.114	0.133	0.128
MgO	4.572	4.585	4.160	4.830	4.868	4.742	3.764	4.014	7.113	6.752	6.15	4.7	5.117	4.665	5.014	5.369	4.448
CaO	0.002	0.000	0.023	0.004	0.009	0.001	0.023	0.006	0.001	0.004	0.008	0.005	0	0.009	0.008	0.018	0.004
Na_2O	0.000	0.000	0.012	0.002	0.039	0.040	0.015	0.069	0.009	0.024	0	0.058	0.016	0.033	0.038	0.052	0.011
K_2O	0.000	0.001	0.001	0.000	0.000	0.000	0.006	0.000	0.003	0	0.002	0	0.018	0	0.007	0.009	0.009
ZnO	0.272	0.343	0.341	0.424	0.310	0.481	0.371	0.000	0.808	0.000	0.000	0.973	0.924	0.896	0.43	0.568	0.614
Total	98.458	96.493	96.556	102.432	104.025	101.991	98.815	98.271	99.645	95.822	98.721	100.218	99.991	99.422	98.859	100.123	99.849
Cation Numbers based on (O) 32																	
Si	0.004	0.005	0.012	0.011	0.011	0.006	0.004	0.021	0.008	0.013	0.027	0.003	0.003	0.004	0.002	0.006	0.012
Ti	0.005	0.003	0.003	0.000	0.009	0.002	0.001	0.002	0.003	0.004	0.006	0.008	0.001	0.005	0.010	0.006	0.004
Al	15.931	15.785	15.860	15.727	15.684	15.910	15.803	15.603	15.520	15.269	15.366	15.566	15.611	15.547	15.663	15.721	15.711
Cr	0.068	0.069	0.054	0.029	0.021	0.014	0.045	0.045	0.002	0.029	0.051	0.074	0.026	0.055	0.048	0.027	0.035
Fe	6.345	6.517	6.549	6.643	6.718	6.427	6.826	7.043	6.182	6.631	6.707	6.721	6.615	6.793	6.599	6.425	6.717
Mn	0.046	0.036	0.041	0.048	0.048	0.033	0.036	0.039	0.000	0.015	0.005	0.036	0.037	0.036	0.022	0.025	0.025
Mg	1.547	1.591	1.443	1.584	1.575	1.552	1.285	1.384	2.378	2.368	2.095	1.586	1.724	1.588	1.703	1.794	1.500
Ca	0.000	0.000	0.006	0.001	0.002	0.000	0.006	0.001	0.000	0.001	0.002	0.001	0.000	0.002	0.002	0.004	0.001
Na	0.000	0.000	0.005	0.001	0.016	0.017	0.007	0.031	0.004	0.011	0.000	0.025	0.007	0.015	0.017	0.023	0.005
K	0.000	0.000	0.000	0.000	0.000	0.000	0.002	0.000	0.001	0.000	0.001	0.000	0.005	0.000	0.002	0.003	0.003
Zn	0.046	0.059	0.059	0.069	0.050	0.078	0.063	0.000	0.134	0	0	0.163	0.154	0.151	0.072	0.094	0.103
Total	23.991	24.065	24.032	24.112	24.135	24.039	24.076	24.168	24.231	24.340	24.259	24.182	24.184	24.197	24.141	24.127	24.115
X_{Mg}	0.196	0.196	0.181	0.193	0.190	0.195	0.158	0.164	0.278	0.263	0.238	0.191	0.207	0.190	0.205	0.218	0.183
X_{Fe}	0.804	0.804	0.819	0.807	0.810	0.805	0.842	0.836	0.722	0.737	0.762	0.809	0.793	0.810	0.795	0.782	0.817

Spinel: The chemical analyses of green spinel of Pavagada area are given in Table VIII along with the structural formula based on 32 (O) atoms. The studied spinels correspond to hercynite variety, with X_{Fe} values vary from 0.72 to 0.84 but X_{Mg} values varies from 0.16 to 0.28. The Al_2O_3 content of the spinel varies from 55.04 – 61.44 wt% and ZnO content varies from 0.27 -0.97wt%.

V. GEOTHERMOBAROMETRY

Geothermobarometry is a technique that utilizes the temperature and pressure dependence of the equilibrium constant (K_{eq}) to infer temperature and pressures of equilibration of mineral assemblages. In metamorphic terrains it can constrain actual P-T paths during metamorphism and in conjunction with geochronology can be used to characterize P-T-t paths, potentially tectonic history. In the present study we were used Garnet-Biotite, Garnet-Cordierite and Garnet-Orthopyroxenes mineral pair exchange thermometers to calculate the temperature conditions of metamorphism at uniform pressure of 5kb for the studied metapelites.

Garnet – Biotite thermometer: The coexistence of garnet-biotite provides a thermometer that has been calibrated from natural assemblages by Thompson 1976 and from experiment by Ferry and Spear 1978. These thermometers are affected by Ca, Mn, Ti and Al^{vi} solution in biotite (and by Ca and Mn solution in garnet) and are believed to be accurate to $\pm50^0$C. The thermometer of Ferry and Spear agrees with that of Thompson to within 50^0C for temperatures below 700^0C, but for T>700^0C, Ferry and Spear's thermometer infers significantly higher temperatures.

Garnet-biotite thermometer is based on Fe-Mg distribution between the two minerals. For the estimation of the peak metamorphic conditions only garnet cores and matrix biotite are used. In this study garnet-biotite geothermometric models of Bhattacharya et al (1992), Dasgupta et al (1991), Perchuk & Lavrent'eva (1983), Ferry and Spear (1978), Holdway and Lee (1977) and Thompson (1976) have been used for calculating temperatures for metapelites of Pavagada & Bandihalli areas and the estimates are listed in the Table IX. The accuracy of these thermometers are claimed to be up to 50^0C.

Garnet-Cordierite thermometer: A Garnet -cordierite thermometer has been calibrated by Well (1979). This is very sensitive to change in X_{Fe} in either phase, and since garnet may not be homogenous, temperatures below peak metamorphism may be recorded. However, peak temperatures from this thermometer have been found to be consistent with other thermometers (Harris and Jayaram 1982). Its calibration is based on the experimental work of Hensen and Green (1971), which was conducted in the hydrous system. More recently, Martignole and Sisi (1981) provide a thermodynamic model for cordierite break-down in the anhydrous system, which reverse the slope on the garnet and cordierite isopleths and thereby provide an alternative garnet-cordierite thermometer more suitable for granulite assemblages which are characterized by low P $_{H2O}$.

Garnet -cordierite thermometer is based on Fe-Mg exchange between co-existing garnet-cordierite assemblages. To assess the temperatures of equilibration of cordierite-garnet assemblages of Pavagada and Bandihalli area, thermometric models proposed by Holdway & Lee (1977) and Thomson (1976) have been attempted. The calculated temperatures produced by these thermometers are listed in the Table IX. The temperatures are calculated using uniform pressure of 5kb. The uncertainty of these thermometers is around $\pm 75^0$C.

Garnet-Orthopyroxene thermometer: The Fe^{2+}-Mg fractionation between garnet and orthopyroxene can be used as a geothemometers for a variety of natural assemblages that have formed at the conditions of the earth's upper mantle and granulite facies metamorphism. The geothermometric relation has been investigated by Dahl (1979), Sen and Bhattacharya (1984), Harley (1984), and Lee and Ganguly (1987). The relationship proposed by Dahl is essentially derived from the thermo compositional dependence of Fe-Mg partition between opx and garnet, while that of Sen and Bhattacharya (1984) is derived using enthalpy and entropy of the Mg and Fe end members of opx and garnet which were either derived from phase equilibrium experimental data or adopted from published thermodynamics data. Harley's (1984) calibration is based primarily on results of synthesis experiments from glasses of appropriate compositions, which do not necessarily represent equilibration to the experimental P-T conditions. Lee and Ganguly (1987) have constrained the equilibrium compositions of coexisting garnet and orthopyroxene in FMAS (FeO-MgO-Al_2O_3-SiO_2) system by reversed experiments between 900^0 and 1400^0 C, and integrated the garnet mixing model of Ganguly and Saxena (1984) to develop a geothermometric expression.

In the present study geothermometric equations developed by Harley (1984), Dhal (1980) and Sen & Bhattacharya (1984) are used. Since the formulations proposed by these authors are compatible with experimentally determined phase equilibria, and low scatter of temperatures. To calculate the temperatures assumed uniform pressure of 5 Kb is used. The results are listed in the Table IX.

Temperature estimation based on Al contents in Orthopyroxene:
Despite the obvious theoretical advantages of garnet-opx Al-solubility-based thermobarometry, Pattison et al., 2003 assessed the temperature of formation of granulites by combining experimental constraints on the P-T stability of granulite facies mineral association with garnet-opx thermobarometry scheme, based on Al solubility in opx, corrected

for late Fe-Mg exchange. Their findings suggest that the P-T conditions of the granulites is underestimated by over 100^0 C. Accordingly an attempt is made to estimate P-T conditions using the method of Pattison et al 2003. The Table X shows changes in inferred P-T conditions for different X_{Al} concentrations in opx (X_{Al}=Al/2), with all other mineral compositions held constant and the other elements in opx varied proportionately. The X_{Al} content of opx of Pavagada area (0.09- 0.15) suggest the corrected Fe-Mg-Al temperature of about 840^0 C and pressure 7.3 kbars where as X_{Al} content of opx of Bidaloti area (0.05-0.07) suggest the corrected Fe-Mg-Al temperature of about 650^0 C and pressure 5.5kbars.

Area Name and rock type			Pavagada metapelites		Bandihalli Metapelite
Sample No.			P-02	P-01	BHA-07
Thermometry	*Garnet-Biotite*		T in ^{0}C		T in ^{0}C
	Thompson 1976		638		560
	Holdway & Lee 1977		615		548
	Ferry & Spear 1978		633		533
	Perchuk & Laurent'va 1983		612		558
	Dasgupta et al 1991		605		558
	Bhattacharya et al 1992				
	HW		618		566
	GS		623		578
	Garnet-Cordierite		T in ^{0}C		T in ^{0}C
	Thompson 1976		654		628
	Holdway & Lee 1977		638		616
	Garnet-Opx		T in ^{0}C		
	Harley 1984		720		
	Dhal 1980		801		
	Sen & Bhattacharya 1984		762		
	Spinel-Cordierite		T in ^{0}C	T in ^{0}C	
	Vielzeuf 1983		870	767	

Table IX. Calculated temperatures based on garnet-biotite, garnet-cordierite, garnet-orthopyroxene and spinel-cordierite pairs for the studied metapelites at 5kb of pressure.

Table X. Variation in uncorrected Fe-Al and corrected Fe-Mg-Al temperatures as a function of Al concentration in orthopyroxene (Pattison et al 2003).

X_{Al}	Wt% Al_2O_3	Uncorrected Fe-Al		Corrected Fe-Mg-Al	
		P (kbar)	*T (^{0}C)*	*P (kbar)*	*T (^{0}C)*
0.15	6.8	9.6	920	9.7	1050
0.13	5.9	8.9	880	8.9	990
0.11	5.0	8.1	840	8.1	920
0.09	4.1	7.3	790	7.3	840
0.07	3.2	6.4	730	6.4	750
0.05	2.2	5.5	670	5.5	650
0.03	1.3	4.3	570	4.3	480

VI. P-T-t PATHS:

Metamorphism, deformation and magmatism make up important factors in an orogeny; their interplay produces strikingly different P-T-t paths. Diversity in P-T-t paths relates to different tectonic settings. Characteristics shape and style of metamorphic P-T-t paths, in particular, may provide important insight into the crustal evolution because these paths may be sensitive monitors of the interplay of tectonic processes and thermal relaxation.

Mainly two types of P-T-t paths are diagnostic, either near isobaric cooling (IBC) or near isothermal decompression (ITD). These P-T-t loops may be either clockwise or counter-clockwise in style. However, in nature, P-T-t paths are often complex and hybrid and may represents a combination of both ITD and IBC, such as an initial IBC followed by ITD (or vice versa) related to multiple tectonothermal events.

Distinguishing between these two types of P-T paths is important because they imply different tectonic scenarios for the origin of granulites. Isothermal decompression paths are generally believed to be representative of crust that has been thickened by tectonic processes and unroofed by either erosion or tectonic denudation (England and Richardson, 1977;

England and Thompson, 1984; Thomson and England, 1984). Tectonic denudation, such as ductile thinning or an extension-related normal fault, results in a steeper decompression path (Fig. 19). Harley (1989) and Anovitz and Chase 1990 argue that some type of tectonic denudation is required to explain the shapes of the P-T paths from granulite terranes that have undergone nearly isothermal decompression.

Isobaric cooling paths are more difficult to interpret unless some portion of the prograde P-T path can be deduced. For example, Bohlen (1987) has argued that isobaric cooling paths indicate that the prograde path was a "counterclockwise" loop (heating accompanied by loading), and has attributed such paths to magma accretion beneath existing continental crust (Fig. 20). However, nearly isobaric cooling paths can also be generated in the deeper portions of thickened terranes that have undergone periods of either rapid erosion or crustal thinning (Fig. 20). Ellis (1987) has argued that granulite facies terranes that display nearly isobaric cooling may have been produced at the base of a doubly thickened crust that has been arrested at mid-crustal levels during the unroofing of the upper crust. The isobaric cooling then occurs as a steady state geotherm is imposed on the post-orogenic crust. A second orogeny is required to uplift and expose the terrane.
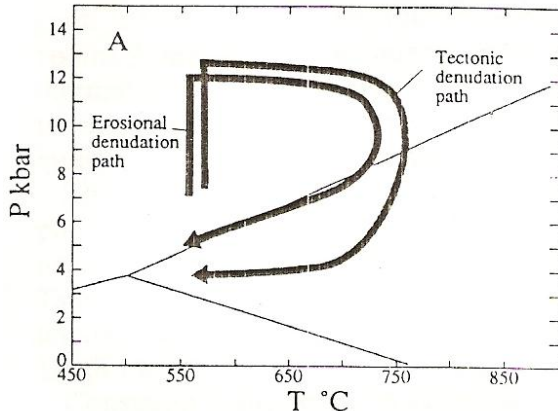
Fig. 19. Schematic P-T paths showing possible Isothermal decompression paths.
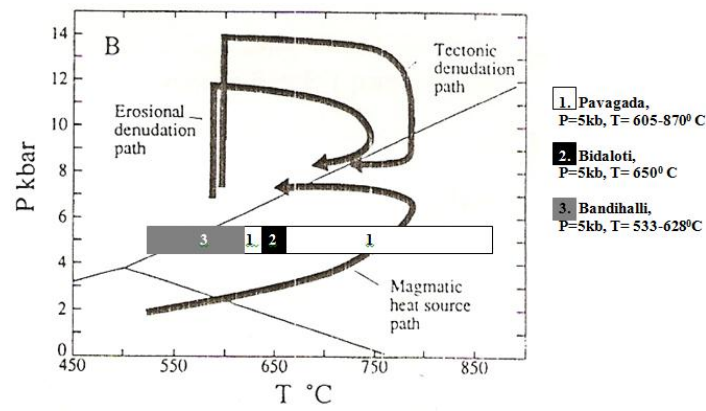
Fig. 20. Schematic P-T paths showing possible Isobaric cooling paths.

The only requirement for the development of a nearly isobaric cooling path is a geotherm that has been elevated above the steady state value. This type of elevated geotherm can readily be produced by either addition of heat to the crust (e.g. by magma accretion) or by crustal thinning. The decay of this perturbed geothermal towards the steady state value, in the absence of unroofing, will result in an isobaric cooling path. It should also be noted that an isobaric cooling path is characteristic of the lower portion of the upper plate of a thrust sheet (e.g. Spear et al., 1984, 1990). Without information on the prograde portions of the paths it will be impossible to distinguish between these very different mechanisms.

In a clockwise P-T-t path, maximum pressure is attained prior to the thermal maxima and they are normally related with plate collision, producing thick crust and moderate to high pressure metamorphic terrains with a thermal imprint. The origin and setting of the regional granulites in relation to the thickening of the crust can be achieved through other possible mechanism;
i.   Crustal thickening by overthrusting (intracontinental, ocean-continent subduction).
ii. Crustal thickening by vertical stretching (continental collision)
iii. Crustal thickening by magmatic accretion (growth of crust from mantle).

It is believed that continental collision provides an effective mechanism for burial, heating, transportation and re-exposure of many granulite grade metamorphic belts in an orogenic event.

Anticlockwise P-T-t paths characterize low P, high T metamorphism, where heating of the crust occurs before and during the tectonic loading such that the thermal maxima are attained prior to the peak-P conditions. Possible heat sources for granulite metamorphism include;
i.   Magmatic heating and heat transport by fluid flow.
ii. Conductive heating in double thickened continental crust.
iii. Conductive heating of thin imbricate thrust slices in the lowermost crust.
iv. Major preheating of the overthrust crust prior to simple shear thrusting.
v.   Shear heating along the thrust.

VII. DISCUSSION AND CONCLUSION

Pavagada Area: The thermobarometry, mineral reactions, deduced on textural criteria, collectively suggest that dehydration-melting of biotite-plagioclase-quartz±sillimanite bearing protoliths of variable composition produced the contrasting peak mineral assemblages in different associations at 750-800^0 C, ~ 5 kbar (equivalent to 18-20km of burial).

We argue that the spinel-cordierite symplectite in association 1 was produced during prograde heating, presumably short-lived (cf. Pitra and Waal, 2001). Evolution of mineral assemblages in association 2 supports a more complete P-T trajectory that involves nearly isobaric heating and cooling that included partial melting, melt extraction and re-introduction of melt. Similarly heating-cooling trajectories have earlier been inferred from HT/UHT metamorphic terranes (Waters, 1989; Dasgupta et al., 1997; Sengupta et al., 1999; Pitra and Waal, 2001). One commonality amongst such terranes is that metamorphism was induced by magmatic intrusions.

Bidaloti area: From the mineral reactions, it is clear that the formation of orthopyroxene may be related to prograde metamorphism, whereas the formation of orthoamphibole is related to hydration reaction and the cordierite formation is seen forming both in the dehydration and hydration reactions. The textural evidence also indicates that these reactions are sliding reactions which are mainly controlled by the variable activities of P_f. Therefore, metamorphic mineral paragenesis clearly point to the fact that the metamorphism must have been initiated at lower P_{H2O} and culminated at higher P_{H2O}, as inferred from the coexistence of orthopyroxene and orthoamphibole and from their textural relationship. Because opx+cord+qtz assemblage is stable at lower P_{H2O} while orthoamphibole-quartz would be common in rocks with higher P_{H2O} (Lal et al, 1984). The absence of almandine garnet in the assemblage indicates that metamorphism is restricted to low pressure conditions. However, the coexistence of orthoamphibole and orthopyroxene with cordierite indicates pressures of 5kb and temperature of 700^0 C if $P_{H2O} < 0.5$ P_{total} and under wetter conditions anthophyllite is the stable phase (Chernosky and Antio, 1979). These mineral assemblages as well as their relationship indicate a near isobaric cooling path of Bidaloti area.

Bandihalli area: The mineral constituents of this locality are more or less same as that of Bidaloti area, with dominance of orthoamphibole, appearance of garnet and absence of orthopyroxene. The assemblage orthoamphibole + aluminosilicate represents relatively high pressure condition, the equivalent low pressure assemblage will be represented by staurolite + cordierite + orthoamphibole at low temperatures and garnet + cordierite + orthoamphibole at higher temperatures. This enables relative evaluation of P-T conditions of several common assemblages (Spear & Schumacher, 1982). Significantly, staurolite is absent in the pelitic assemblages of Bandihalli. Thus in the assemblages where staurolite is absent, coexistence of garnet and cordierite represent relatively intermediate pressure and high-temperature conditions of the medium grades of upper amphibolite-granulite facies, where coexistence of sillimanite and k-feldspar are absent. The pelites of Bandihalli clearly show two generations of orthoamphibole. From textural evidence, it is clear that the anthophyllite is of the first generation, whereas gedrite is of second generation. The P-T estimates obtained are 5kb and 530-630^0 C, which indicate that the area has undergone upper amphibolite-low granulite facies condition of metamorphism. The overall mineral assemblages as well as their relationship indicate a near isobaric cooling path.

Overall the present study suggests that there is no increase in grade of metamorphism from north to south, at least in the EDC based on thermobarometry, petrography, mineral assemblages, mineral reactions and mineral chemistry. In Central part (Pavagada area) of EDC itself we are getting HT-UHT assemblages with an estimated temperature of 750-845^0 C at ~5kbar of pressure, which was considered earlier as green schist to lower amphibolite facies domain. Bidaloti metapelites yields a temperature of 600-700 ^{0}C at an assumed pressure of 5kb by using different set of thermometers whereas Bandihalli area metapelites yields a temperature of 530-630^0 C at an assumed pressure of 5kb.

ACKNOWLEDGMENT

REFERENCES

[1] Anantha Iyer, G.V. and Narayana Kutty, T.R. (1974) Geochemistry of garnets from the Precambrian of South Karnataka. Geol. Soc. India, 15, 256-269.

[2] Bhattacharya, A., Mohanty, L., Maji, A., Sen, S.K., and Raith, M. (1992) Non-ideal mixing in the phlogopite-annite boundary: Constraints from experimental data on Mg-Fe partitioning and a reformulation of the biotite-garnet geothermometer. Contributions to Mineralogy and Petrology, 111, 87–93.

[3] Bohlen, S.R. (1987) Pressure-temperature-time paths and a tectonic model for the evolution of granulites. Jour. Geology, v.24, pp.617-632.

[4] Bouhallier, H. (1995) Evolution structurae et metamorphic de la croute continentale archeenne (cratin de Dharwar Inde du sud) in: Mem. Doc., Geoscienes Rennes vol, 60. 277p.

[5] Chardon, D and Jayananda, M (2008a) A 3D field perspective on deformation, flow and growth of the lower continental crust. Tectonics, v. 27, TC1014, doi: 10. 1029/2007 TC002120, American Geophysical Union.

[6] Chardon, D., J.-J. Peucat, M. Jayananda, P. Choukroune, and C. M. Fanning (2002) Archean granite-greenstone tectonics at Kolar (South India): interplay of diapirism and bulk inhomogeneous contraction during magmatic juvenile accretion, Tectonics, 21, 10.1029/2001TC901032.

[7] Chardon, D., Jayananda, M., Chetty, T.R.K., Peucat, J-J (2008b) Precambrian continental strain and shear zone patterns: the South Indian case. Journal of Geophysical Research-Solid Earth doi: 10.1029/2007JB005299 American Geophysical Union.

[8] Chernosky, J.V and Antio, L.K. (1979) The stability of anthophyllite in the presence of quartz. Amer. Mineral., 64, 294-303.

[9] Dahl, P (1979) Comparative geothermometry based on major element and oxygen isotope distributions in Precambrian metamorphic rocks from southwestern Montana: American Mineralogist, 64, 1280-1293.

[10] Dahl, P.S. (1980) The thermal-compositional dependence of Fe^{2+}-Mg distributions between coexisting garnets and pyroxenes; applications to geothermometry: Am. Min., v. 65, p. 852-866.

[11] Das, K., Bose, S., Ohnishi, I., Dasgupta, S. (2006) Garnet-spinel intergrowths in ultrahigh-temperature granulite, Eastern Ghats, India: possible evidence of an early Tschermak-rich orthopyroxene during prograde metamorphism. Am. Mineral., 91, 375-384.

[12] Dasgupta, S., Ehl, J., Raith, M.M., Sengupta, P., Sengupta, P. (1997) Midcrustal contact metamorphism around the Chimakurthy mafic–ultramafic complex, Eastern Ghats Belt, India. Contributions to Mineralogy and Petrology 129, 182–197.

[13] Dasgupta, S., S. Sengupta, D. Guha and M. Fukuoka (1991) A refined garnet-biotite Fe-Mg exchange geothermometer and its application in amphibolites and granulites. Contrib. Mineral. Petrol., 130-137.

[14] Dymek, R.F. (1983) Titanium, aluminium and interlayer cation substitutions in biotite from high-grade gneisses, West Greenland. Amer. Mineral., 68, 880-899.

[15] Ellis D. J. (1987) Origin and evolution of granulites in normal and thickened crusts; Geology 15, 167–170.

[16] England, P.C. and Richardson, S.W (1977) The influence of erosion upon the mineral facies of rocks from different metamorphic environments. Journal of the Geological Society of London, 134, 201-213.

[17] England, P.C. and Thompson, A.B. (1984) Pressure-temperature-time paths of regional metamorphism. I. Heat transfer during the evolution of regions of thickened continental crust. Journal of Petrology, 25, 894-928.

[18] Ferry, J.M. and Spear, F.S. (1978) Experimental calibration of the partitioning of the Fe and Mg between biotite and garnet. Contrib. Mineral. Petrol., 66, 113-117.

[19] Friend, C.R.L. and Nutman, A.P. (1992) Response of U-Pb isotopes and whole rock geochemistry to Co2 induced granulite metamorphism, Kabbaldurga, Karnataka south India. Contrib. Mineral. Petrol, 111, 299-310.

[20] Ganguly, J. and Saxena, S.K. (1984) Mixing properties of aluminosilicate garnets: constraints from natural and experimental data, and applications to geothermo-barometry. Am. Miner., 69, 88-97.

[21] Hansen, E. C., R. C. Newton, and S. Janardhan (1984a) Pressures, temperatures and metamorphic fluids across an unbroken amphibolite facies to granulite facies transition in southern Karnataka, India, in Archaean geochemistry, edited by A. Kröner and A. M. Goodwin, pp. 160-181, Springer-Verlag, Berlin.

[22] Hansen, E. C., R. C. Newton, and S. Janardhan (1984b) Fluid inclusions in rocks from the amphibolite-facies gneiss to charnockite progression in southern Karnataka, India: direct evidence concerning the fluids of granulite metamorphism, J. Metam. Geol., 2, 249-264.

[23] Harley S L (1989) The origin of granulites: A metamorphic perspective; Geol. Mag. 126, 215–247.

[24] Harris, N.B.W. and Jayaram, S. (1982) Metamorphism of cordierite gneisses from the Bangalore region of the Indian Archean. Lithos 15, 89-98.

[25] Hensen, B.J and Green, D.H. (1971) Experimental study of the stability of cordierite and garnet in pelitic compositions at high pressures and temperatures. I. Compositions with excess alumino-silicate. Contrib. Mineral. Petrol., 33, 309-330.

[26] Holdaway, M.J and Lee, S.M. (1977) Fe-Mg cordierite stability in high-grade politic rocks based on experimental, theoretical and natural observations. Contrib. Mineral. Petrol., 63, 175-198.

[27] Hormann, P.K., Raith, M., Raase, P., Ackermand, D. and Seifert, F (1980) The granulite complex of Finnish Lapland: Petrology and metamorphic conditions in the Ivalojoki-Inarijarvi area; Geol. Surv. Finland Bull., v.308, pp.1-55.

[28] Janardhan, A. S., R. C. Newton, and E. C. Hansen (1982) The transformation of amphibolite facies gneisses to charnockite in southern Karnataka and Tamil Nadu, Contrib. Mineral. Petrol., 79, 139-149.

[29] Jayananda, M., Moyen, J.-F., Martin, H., Peucat, J.-J., Auvray, B., Mahabalesawar, B. (2000) Late Archaean (2550–2520 Ma) juvenile magmatism in the Eastern Dharwar craton, southern India: constraints from geochronology, Nd–Sr isotopes and whole rock geochemistry. Precambrian Research, 99, 225–254.

[30] Jayananda, M., H. Martin, J.-J. Peucat, and B. Mahabaleswar (1995) Late Archaean crust-mantle interactions: geochemistry of LREE-enriched mantle derived magmas. Example of the Closepet batholith, Southern India, Contrib. Mineral. Petrol., 119, 314-329.

[31] Krogstad, E.J,. Hanson, G.N. and Rajamani, V, (1991). U-Pb ages of zircon and sphene for two gneiss terranes adjacent to the Kolar Schist Belt, South India: evidence for separate crustal evolution histories. J. Geol. 99, 801-816.

[32] Leake, B.E. (1978) Nomenclature of Amphiboles. Mineral.Magazine., v.42, pp.533-63.

[33] Lee, H and Ganguly, J (1987) Equilibrium compositions of coexisting garnet and orthopyroxene: experimental determinations in the system FeO-MgO-Al2O3-SiO2 and applications. Jour. Petrol., 29, 93-114.

[34] Martignole, J and Sisi, J.C. (1981) Cordierite-Garnet-H2O equilibrium: a geological thermometer, barometer and H2O fugacity indicator. Contrib. Mineral. Petrol., 77, 38-46.

[35] Miyashiro, A (1957) Cordierite-indialite relations. Am. Jour. Sci., 255 : 43-62.

[36] Nutman, A.P., Chadwick, B., Krishna Rao, B. and Vasudev, V.N. (1996) SHRIMP U/Pb zircon ages of acid volcanic rocks in the Chitradurga and Sandur groups, and granites adjacent to the Sandur Schist belt, Karnataka. J. Geol. Soc. India. 47, 153-164.

[37] Pattison, D.R.M., Chacko, T., Farquhar, J., McFarlane, C.R.M. (2003) Temperatures of granulite facies metamorphism: constraints from experimental phase equilibria and thermometry corrected for retrograde exchange. Jour. Petrol., 44, 867-900.

[38] Perchuk, L.L. and Lavrent'eva (1983) Experimental investigation of exchange equilibria in the cordierite-garnet-biotite, Kinetics and equilibrium in mineral reactions, ed. By S.K. Saxena. New York, Springer, 199-239 (Advances in Physical Geochemistry, v. 3).

[39] Peucat, J.J., Mahabaleswar, B. and Jayananda, M. (1993) Age of younger tonalitic magmatism and granulitic metamorphism in the south India transition zone (Krishnagiri area): Comparison with older Peninsular gneisses from the Gorur-Hassan area. J. Metamorphic. Geol. 11,879-888.

[40] Pichamuthu, C.S. (1985) Chitradurga Schist Belt , Jour. Geol. Soc. India, v. 26, pp. 509-510.

[41] Pitra, P and De Wall S.A. (2001) High-temperature, low pressure metamorphism and development of prograde symplectites, marble Hall fragment, Bushveld Complex (South Africa). J. Metam. Geol., 19, 311-325.

[42] Raase, P, Raith M, Ackermand, D and Lal, R.K. (1986) Progressive metamorphism of mafic rocks from greenschist to granulite facies in the Dharwar craton of South India; Jour. Geol., 94, 261-282.

[43] Radhakrishna, B.P. (1984) Crustal evolution and metallogeny-evidence from the Indian shield. Jour. Geol., 94, 145-166.

[44] Raith, M., Raase, P., Ackermand, D. and Lal, R.K. (1982) The Archean Dharwar craton of Southern India: metamorphic evolution and P-T conditions. Geol. Runds., v.71, pp.280-290.

[45] Rama Rao, B. (1936) Recent investigations on the Archaean complex of Mysore. Proc. Indian Sci. Congr. Presidential address to geology and geography section, 215-244.

[46] Rollinson, H. R., Windley, B. F., Ramakrishnan, M. (1981) Contrasting high and intermediate pressures of metamorphism in the Archaean Sargur Schists of southern India: Contrib. Mineral. Petrol, 76, 420-429.

[47] Sen SK, Bhattacharya A (1984) An orthopyroxene–garnet thermometer and its application to the Madras charnockites. Contrib Mineral Petrol 88:64–71.

[48] Sengupta, P., Sen, J., Dasgupta, S., Raith, M., Bhui, U.K., Ehl, J. (1999) Ultrahigh temperature metamorphism of metapelitic granulites from Kondapalle, Eastern Ghats Belt: implications for the Indo-Antarctic correlation. J. Petrol. 40, 1065–1087.

[49] Spear F.S. and Schumacher J.C. (1982) Orthoamphibole and cummingtonite amphibolites. In : Veblen DR, Ribbe PH (eds) Amphiboles: petrology and experimental phase relations (Reviews in Mineralogy, vol 9B) Mineralogical Society of America, Chelsea, Michigan, pp 159 182.

[50] Spear, F.S., Kohn, M.J., Florence, F.P. and Menard, T., 1990. A model for garnet and plagioclase growth in pelitic schists: implications for thermobarometry and P-T path determinations. J. Metamorph. Geol., 8: 683-696.

[51] Spear, F.S., Selverstone, J., Hickmott, D., Crowley, P., Hodges, K.V. (1984) P-T paths from garnet zoning: a new technique for deciphering tectonic processes in crystalline terrains. Geology, 12, 87-90.

[52] Swami Nath, J., Ramakrishnan, M. (1981) Early Precambrian supracrustals of southern Karnataka. Mem. Geol. Surv, India, 112, 328.

[53] Swami Nath, J., Ramakrishnan, M. and Viswanatha, M.N. (1976) Dharwar stratigraphic model and Karnataka craton evolution. Geol. Surv. India records. 107,149-175.

[54] Thompson, A.B. (1976) Mineral reactions in politic rocks. II. Calculation of some P-T-X (Fe-Mg) phase relations. Am. J. Sci., 276, 401-454.

[55] Thompson, A.B. and England, P.C. (1984) Pressure-temperature-time paths of regional metamorphism II. Their inference and interpretation using mineral assemblages in metamorphic rocks. Journal of Petrology, 25, 929-955.

[56] Waters, D. J. (1989) Metamorphic evidence for the heating and cooling path of Namaqualand granulites. In: Evolution of Metamorphic belts (eds Daly, J.S., Cliff, R.A and Yardley, B.W.D.), Special publication of the Geological Society, London, 43, 357-363.

[57] Wells, PR.A. (1979) Chemical and thermal evolution of Archaean sicilic crust, Southern West Greenland. Journal of Petrology, 20, 187-226.